

# **A summary of the geology, geochemistry, and geophysics of the Roosevelt Hot Springs thermal area, Utah**

S. H. WARD , W. T. PARRY , W. P. NASH , W. R. SILL ,  
K. L. COOK , R. B. SMITH , D. S. CHAPMAN ,  
F. H. BROWN , J. A. WHELAN , AND J. R. BOWMAN

## A summary of the geology, geochemistry, and geophysics of the Roosevelt Hot Springs thermal area, Utah

S. H. WARD\*, W. T. PARRY\*, W. P. NASH\*, W. R. SILL\*,  
K. L. COOK\*, R. B. SMITH\*, D. S. CHAPMAN\*,  
F. H. BROWN\*, J. A. WHELAN\*, AND J. R. BOWMAN\*

The Roosevelt Hot Springs thermal area is a newly discovered geothermal power prospect in Utah. Seven production wells have been drilled with a maximum per well flow capability averaging  $4.5 \times 10^5$  kg of combined vapor and liquid per hour at a shut-in bottom hole temperature near 260°C.

The thermal area is located on the western margin of the Mineral Mountains, which consist dominantly of a Tertiary granitic pluton 32 km long by 8 km wide. Rhyolitic tuffs, flows, and domes cover about 25 km<sup>2</sup> of the crest and west side of the Mineral Mountains within 5 km of the thermal area. The rhyolitic volcanism occurred between 0.8 and 0.5 m.y. ago and constitutes a major Pleistocene thermal event believed to be significant to the evaluation of the Roosevelt Hot Springs thermal area. Thermal waters of the (now) dry spring, a seep, and the deep reservoir are dilute (ionic strength 0.1 to 0.2) sodium chloride brines.

Spring deposits consist of siliceous sinter and minor sulfur. Alluvium is cemented by sinter and altered in varying degrees by hot, acid-sulfate water to opal and alunite at the surface, grading successively to alunite-kaolinite, alunite-kaolinite-montmorillonite, and muscovite-pyrite within 60 m of the surface. Observed alteration and water chemistry are consistent with a model in which hot aqueous solutions containing H<sub>2</sub>S and sulfate convectively rise along major fractures. Hydrogen sulfide oxidizes to sulfate near the surface decreasing the pH and causes alunite to form. Opal precipitates as the solutions cool. Kaolinite, muscovite, and K-feldspar are formed in sequence, as the thermal water percolates downward and hydrogen ion and sulfate are consumed.

Major swarms of earthquakes occur 30 km to the

east-northeast near Cove Fort, Utah, but only minor earthquake activity occurs near the Roosevelt Hot Springs thermal area. Delayed *P*-wave traveltimes generated from the Cove Fort microearthquakes, and observed west of the northern Mineral Mountains, are suggestive of a low velocity zone beneath the Mineral Mountains; the vertical and lateral resolution of the data is inadequate to delineate the zone. Gravity and magnetic surveys are useful in determining the structure and depth of valley fill of the area of the northern Mineral Mountains, but neither one has detected an igneous intrusive source of heat. Thermal gradient measurements that range up to 960°C/km in 30 to 60 m deep holes outline a 6 by 12 km thermal field. Heat flow and resistivity data both outline anomalous zones along a system of faults that controls the near-surface fluid flow. The source of heat is interpreted to be the convective circulation of thermal water. The lowered resistivity is due to the hot brine and the associated hydrothermal alteration. Magnetotelluric data are highly anomalous over the field but means for their quantitative interpretation are unavailable at present; the anomalous data could as readily be interpreted as due to surface conductors as deep conductors which one might like to associate with a source of heat.

Any current model of the subsurface is highly speculative but can be expected to improve once existing seismic refraction and magnetotelluric data are fully interpreted. Then multiple-data-set modeling, combined with subsurface control from existing wells, should result in a reasonable model of the geothermal system. This modeling will be aided also by hydrologic, isotopic, structural, and additional *P*-wave delay studies currently in progress.

Manuscript received by the Editor June 1, 1978.

\*Dept. of Geology and Geophysics, University of Utah, Salt Lake City, UT 84112.

0016-8033/78/1201-1515\$03.00. © 1978 Society of Exploration Geophysicists. All rights reserved.

Based upon this case history, an exploration sequence appropriate to the eastern Basin and Range province should consist of phase 0, a digest and synthesis of available data; phase 1, a regional air-photo accumulation and analysis; phase 2, regional geologic mapping, regional radiometric dating of all intrusive and extrusive rocks, regional isotopic and chemical analysis of waters, regional aeromagnetic and gravity surveys, and regional collection of thermal gradients in available holes; phase 3, heat

flow measurements in strategically located holes; phase 4, dipole-dipole resistivity surveys; phase 5, petrological, mineralogical, and geochemical studies on cuttings and cores from heat flow drill holes; phase 6, model test drilling accompanied by petrological, chemical, and isotopic analyses of cuttings and cores plus chemical and isotopic analyses of fluids; phase 7, detailed seismic refraction and reflection surveys; and phase 8, modeling and synthesis of all available data.

## INTRODUCTION

This paper presents a summary of progress to early 1978 of research on the geology, geochemistry, and geophysics of the Roosevelt Hot Springs thermal area, located 19 km northeast of Milford, Utah (Figure 1). The modules used in the investigation of the area are listed in Table 1. Detailed reports, including preliminary numerical modeling and interpretation for each module, are either completed or are in preparation. Those completed include Ward and Crebs, 1975; Crebs and Cook, 1976; Dedolph and Parry, 1976; Geotronics Corp., 1976; Nash, 1976; Olson and Smith, 1976; Parry et al, 1976; Ward and Sill, 1976a; 1976b; Brown, 1977; Brumbaugh and Cook, 1977; Bryant and Parry, 1977; Evans, 1977; Micro-Geophysics Inc., 1977; Sill and Bodell, 1977; Smith, 1977; Ward, 1977; Carter and Cook, 1978; Evans and Nash, 1978; Sill and Ward, 1978; and Wannamaker, 1978. The reader is referred to these voluminous reports for substantiation of necessarily terse statements made in this summary paper; all reports are available from the Department of Geology and Geophysics, University of Utah.

Discharge from the Roosevelt Hot Springs (Figure 2) was 38 l/min at 88°C in 1908, 4 l/min at 85°C in 1950, and "small" at 55°C in 1957. In 1966 the spring was dry (Mundorff, 1970). A small seep with a temperature of 25°C exists nearby today. Concerted industrial geothermal exploration began in 1972. Thermal gradient holes were drilled beginning in 1973 and deeper exploration test drilling, begun in 1975, resulted in the discovery of a potentially commercial thermal reservoir by Phillips Petroleum Co. The area is currently being explored for commercial power production, and three companies have drilled seven production wells and four nonproductive wells. Flow tests indicate potential production of fluids of about  $4.5 \times 10^5$  kg/hr per well at shut-in bottom hole temperatures near 260°C.

We began our research in the area in June 1975.

The purposes of our research are (a) development of a complete case study of the area, (b) delineation of the reservoir and its source of heat, (c) development and/or assessment of technologies suited to exploration for geothermal fields typical of the eastern Basin and Range province, and (d) development of exploration procedures suited to detection and delineation of similar geothermal fields in the eastern Basin and Range province. In this manuscript we describe our efforts, to date, under objectives (a), (b), and (d). Specific documents describing our efforts under objective (c) will appear elsewhere.

## GEOLOGY AND GEOCHEMISTRY

### Introduction

The Roosevelt Hot Springs thermal area is situated near the eastern margin of the Basin and Range province in an area where igneous activity has occurred repeatedly during the past 30 m.y. Late Cenozoic volcanism is common along the edge of the Basin and Range physiographic province in Utah, and the Roosevelt Hot Springs thermal area is one of four Known Geothermal Resource Areas (KGRAs) there (Figure 1). The rock types associated with these KGRAs are high silica rhyolite and basalt or basaltic andesite, the bimodal association characteristic of the province in the late Cenozoic.

The Roosevelt Hot Springs thermal area is located on the western margin of the Mineral Mountains which include the Tertiary granitic Mineral Mountains pluton, schists, and gneisses of indeterminate age, Cretaceous and Paleozoic sedimentary rocks, Tertiary volcanic rocks, and Quaternary rhyolite flows, domes and ash deposits (Figure 2). The granitic

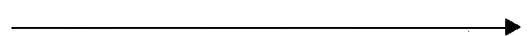
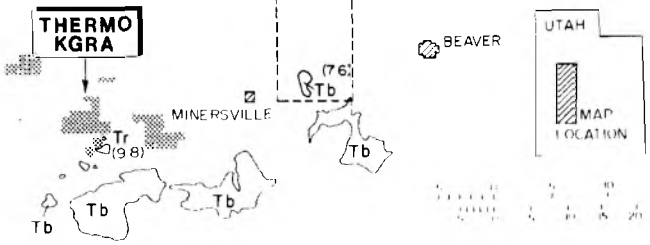
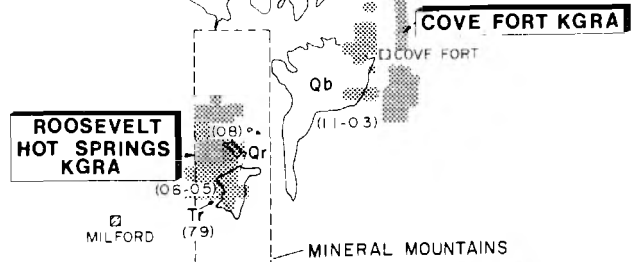
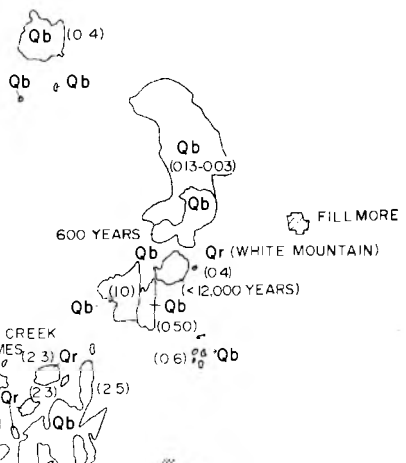
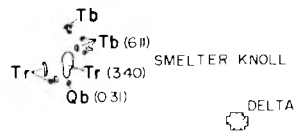
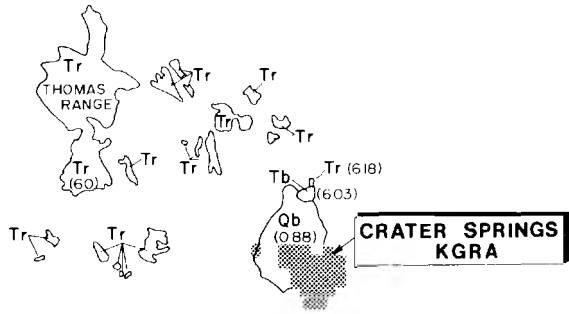


FIG. 1. Distribution of late Tertiary and Quaternary volcanic rocks in west-central Utah. Ages in millions of years. Qb = Quaternary basalt, Qr = Quaternary rhyolite, Tb = Tertiary basalt, Tr = Tertiary rhyolite.

HONEYCOMB HILLS

Tr (47)



BLACK MOUNTAINS

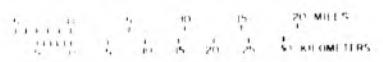


Table 1. Geoscientific methods used at Roosevelt Hot Springs thermal area.

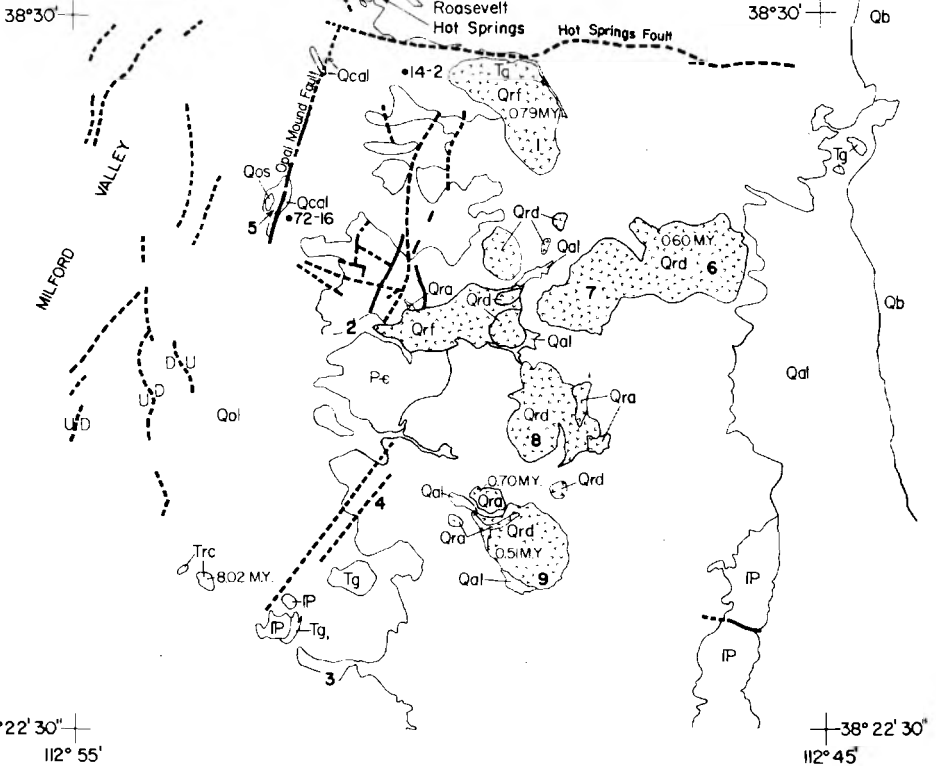
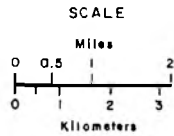
Geology	Geochemistry	Geophysics
Photogeology Low sun-angle, black & white High sun-angle, stereo color photography Orientation survey, multispectral infrared	Mapping and analysis of surficial alteration	Gravity survey
Reconnaissance mapping	Analysis of subsurface alteration	Precise leveling and gravity
Volcanic stratigraphy and mapping	Chemistry of waters	Magnetic survey
Volcanic and plutonic geochronology	Mapping and analysis of surficial deposits	Aeromagnetic survey
Volcanic paleomagnetism	Orientation survey, mercury in soils	Resistivity surveys Schlumberger Dipole-dipole
Magma thermodynamic studies	Orientation survey, $\gamma$ -ray spectrometry	Induced-polarization survey
Physical and kinematic studies of magmas	Assessment of contribution of exothermic reactions to heat flow	Misc-a-la-masse resistivity survey
Chemistry of volcanic rocks and minerals	Development of mass transfer geothermometer	AMT/MT survey
Structural mapping	Stable isotope studies of waters	Electromagnetic sounding Orientation self-potential tests Earthquake monitoring Detailed short-term Long-term Refraction seismic survey Thermal gradients and heat flow Simultaneous modeling of several data sets

FIG. 2. Generalized geologic map of the northern Mineral Mountains, Utah. Quaternary rhyolites are stippled. 1, Bailey Ridge; 2, Wildhorse Canyon; 3, Corral Canyon; 4, Ranch Canyon; 5, Opal Mound; 6, Bearskin Mountains; 7, Little Bearskin Mountain; 8, North Twin Flat Mountain; 9, South Twin Flat Mountain.

EXPLANATION

QUATERNARY	Qal	Alluvium
	Qcal	Cemented Alluvium
	Qos	Opal & Opaline Sinter
	Qb	Basaltic Cinder & Flows
	Qrd	Rhyolite Domes
TERTIARY	Qra	Rhyolite Ash
	Qrf	Rhyolite Flows
	Trc	Rhyolite Domes, Corral Canyon
PALEOZOIC	Tg	Granitic Rocks
	IP	Permian Sedimentary Rocks
PRECAMBRIAN	-ε	Cambrian Sedimentary Rocks
	pε	Precambrian Rocks

--- Faults  
 0.60 M.Y. = K/Ar ages in millions of years  
 72-16 = Drill hole Location



pluton is the largest in Utah (approximately 250 km<sup>2</sup>) and is no older than 35 m.y. (Lipman et al., 1977).

K-Ar dates of 14.0 m.y. (Armstrong, 1970) and 9.4 m.y. (Park, 1971) suggest the pluton is the youngest in Utah. Additional dates of 12.6, 11.8, 10.7, 10.5, and 10.0 m.y., which we have obtained, indicate the K-Ar age of the pluton decreases systematically from north to south. The dominant unit of the pluton is a light colored medium to very coarse grained granite, rich in alkali feldspar and poor in ferromagnesian minerals. In the northern portion of the area, a hornblende biotite granodiorite predominates. Both types are gradational to a darker, fine to medium grained granitic unit. The pluton is cut by mafic and aplitic dikes, and porphyritic rhyolite.

Cretaceous, Triassic, and Permian sedimentary rocks are exposed on the south flank of the pluton, and Cambrian sedimentary rocks are in fault contact to the north. Amphibolite-facies schist and gneiss are exposed along the western margin of the pluton. Although a Precambrian age has been assigned to them in the past, a K-Ar date of 10.5 m.y. indicates that they could have been formed contemporaneously with the main body of the pluton, or that the K-Ar age for the gneiss and schist was reset at 10.5 m.y.

## Volcanism

The Mineral Mountains area has been the site of repeated volcanism. Mid-Tertiary volcanic activity occurred about 20 m.y. ago, and calc-alkalic lavas are exposed on the south flank of the Mineral Mountains and in the Black Mountains which are about 40 km south of Roosevelt Hot Springs, adjacent to the Thermo KGRA (Figure 1). Near the Thermo KGRA, rhyolite dated at 9.7 m.y. was erupted, and to the north, on the western flank of the Mineral Mountains, 8.0 m.y. old rhyolite that overlies granitic alluvium derived from the Mineral Mountain pluton is exposed in Corral Canyon. Basalt dated at 7.6 m.y. occurs on the southern flank of the Mineral Mountains, near the Minersville reservoir (Figure 1) and rhyolite dated at 2.3 m.y. occurs 25 km north of the Roosevelt Hot Springs (Lipman et al., 1977).

The youngest episode of volcanism began about 0.8 m.y. ago with the eruption of two rhyolite flows from vents located about 4 km east of the present near-surface thermal activity. These flows, along Bailey Ridge and Wildhorse Canyon, are about 3 km in length and 80 m thick. The bases of the flows consist of black flow-layered obsidian, whereas the interior is gray devitrified rhyolite. Some obsidian is

Table 2. Chemical analyses of representative rhyolites.

Weight %	Bailey Ridge flow 74-3A	N. Twin Flat Mountain dome 75-20	Corral Canyon rhyolite 75-30
SiO <sub>2</sub>	76.52	76.45	70.13
TiO <sub>2</sub>	0.12	0.08	0.32
Al <sub>2</sub> O <sub>3</sub>	12.29	12.79	14.14
Fe <sub>2</sub> O <sub>3</sub>	0.31	0.30	0.68
FeO	0.46	0.29	1.25
MnO	0.05	0.10	0.02
MgO	0.08	0.12	0.58
CaO	0.64	0.40	2.02
Na <sub>2</sub> O	3.80	4.39	3.44
K <sub>2</sub> O	5.24	4.73	4.58
P <sub>2</sub> O <sub>5</sub>	0.02	0.06	0.12
H <sub>2</sub> O <sup>+</sup>	0.12	0.10	2.07
H <sub>2</sub> O <sup>-</sup>	0.06	—	0.24
F	0.16	0.44	0.09
Sum	99.87	100.25	99.68
Less O = F	0.07	0.19	0.04
Total	99.80	100.06	99.64
ppm			
Ba	130	—	750
Ce	60	40	70
La	45	35	45
Rb	195	340	120
Sr	35	—	270
Zr	100	90	110
Nb	25	35	—

Major element analyses by wet chemical techniques, trace elements by X-ray fluorescence. Analyst, S. H. Evans, Jr.

exposed in the upper portion of the flow. The top consists of perlitic pumice rubble. The rhyolite is almost entirely glass containing less than 1 percent phenocrysts of alkali feldspar, biotite, and Fe-Ti oxides. These flows have reversed magnetic polarities.

Subsequent activity from about 0.6 to 0.5 m.y. ago produced at least ten rhyolite domes and small flows of rhyolite distributed over 15 km along the crest and western flank of the Mineral Mountains. The domes range from about 0.3 to 1 km in diameter and are up to 250 m high. They characteristically have a basal vitrophyre 5 to 10 m thick which grades upward into a gray devitrified rhyolite containing abundant lithophysal cavities. On many of the domes original frothy perlite carapace is still present. The domes exhibit steeply dipping flow layering and ramp structures which are not present in the more fluid earlier lava flows. The formation of domes was preceded by pyroclastic eruptions which produced air-fall and ash-flow tuffs which are best exposed in Ranch Canyon. The dome-forming rhyolites contain up to 10 percent phenocrysts of plagioclase and alkali feldspar, quartz, biotite, Fe-Ti oxides, sphenc, zircon, apatite, and allanite. Topaz occurs in lithophysae in crystalline rhyolite. The ash deposits and domes have normal magnetic polarities.

Quaternary basalt was erupted from two vents on the northeast flank of the Mineral Mountains, and flows from the extensive Cove Fort basaltic-andesite field lap against the Mineral Mountains on the east.

Representative chemical analyses indicate that the Quaternary flows and domes are high silica rhyolites (76.5 percent) and contain over 9 percent total alkalis (Table 2). There are chemical differences between the two magma types: the earlier crystal-poor flows contain relatively more potassium, titanium, iron, calcium, barium, and strontium, whereas the crystal-rich domal rhyolites contain relatively more magnesium, manganese, sodium, fluorine, niobium, and rubidium. The Tertiary rhyolite contains less silica and more calcium, and is strongly enriched in strontium and barium compared to both varieties of Quaternary lavas. One striking feature of the Quaternary lavas is the large compositional range of feldspars precipitated from liquids of similar composition. This is best illustrated by Figure 3 which shows bulk rock and glass compositions together with all the feldspar determinations for both Tertiary and Quaternary rhyolites. If the Tertiary rhyolite data are deleted (crosses), the feldspar compositional range is not as extensive, but is nevertheless considerable. For the lavas studied here, it is evident that small differences

in magma composition, and perhaps temperature, can produce substantial compositional differences in feldspar.

Pre-eruption magma temperatures have been determined using both the iron-titanium oxide and the two-feldspar thermometers. Temperatures range from a high of 785°C in the flows to a low of 650°C in the domes. These temperatures suggest that the magmas contained substantial water and fluorine. Water fugacities calculated for the flows and domes are 3.0 kb and 0.4 kb, respectively (Nash and Evans, 1977).

The chemical and mineralogical data indicate that the dome-forming magma may have been derived from the earlier magma (which gave rise to the flows) by the fractionation of feldspar. The evidence does not preclude the separate generation of each magma batch, or alternatively, derivation of one from the other by chemical gradients as postulated for the Long Valley, California magma system (Hildreth, 1977). The striking chemical similarity of all the domes strongly suggests that they were derived from the same magma batch between 0.6 and 0.5 m.y.

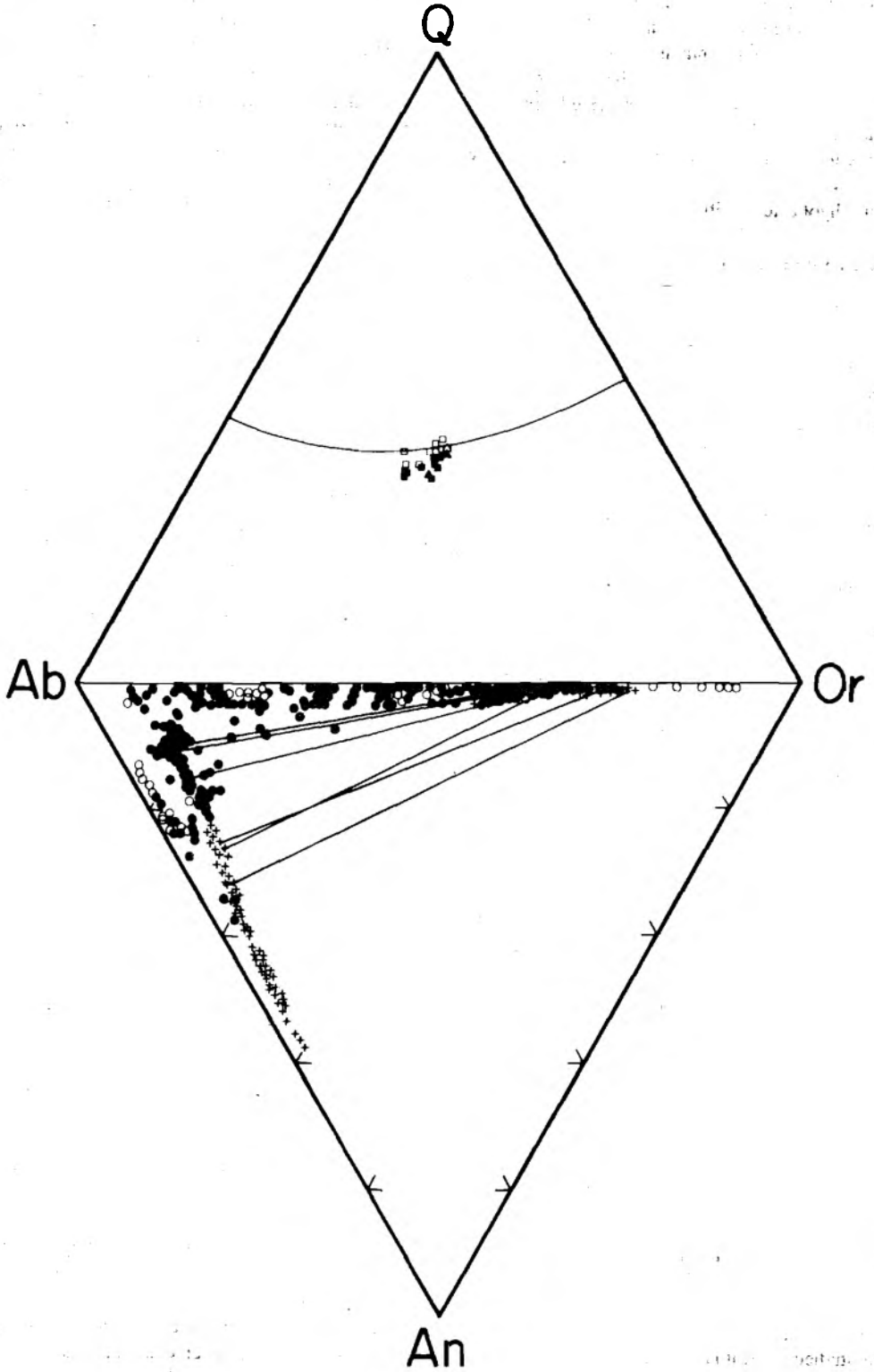
### Spring deposits and alteration

Hot spring deposits consist of siliceous sinter and minor sulfur. Thin horizontally bedded, dense, varicolored opaline sinter produced as a result of primary deposition of silica on broad spring aprons occurs in the Opal Mound area (Figure 2), where laminated, knobby, and colloform opal also occur. Laminations dip steeply to vertically within old spring vents exposed along the Opal Mound fault. Very porous, cellular opaline sinter occurs in minor amounts on the Opal Mound and north of Hot Springs wash. Sinter-cemented alluvium surrounds the spring vents and constitutes a transition between altered alluvium and spring deposits.

Coarsely crystalline granite grading to quartz monzonite of Tertiary age, and alluvium have been hydrothermally altered in the Roosevelt Hot Springs thermal area (Figure 2). The alluvium consists of mineral and rock fragments derived from granite and volcanic rocks of the Mineral Range which have been cemented by opal and chalcedony. Feldspars have been altered by acid-sulfate water to alunite, opal, and hematite. Native sulfur occurs as very fine to coarse euhedral to anhedral intergranular crystals. Micro-crystalline sulfur is intergrown with alunite. Cubic pseudomorphs of hematite after pyrite are also present.

Altered rocks have been sampled in three shallow drill holes. Altered and cemented alluvium overlies





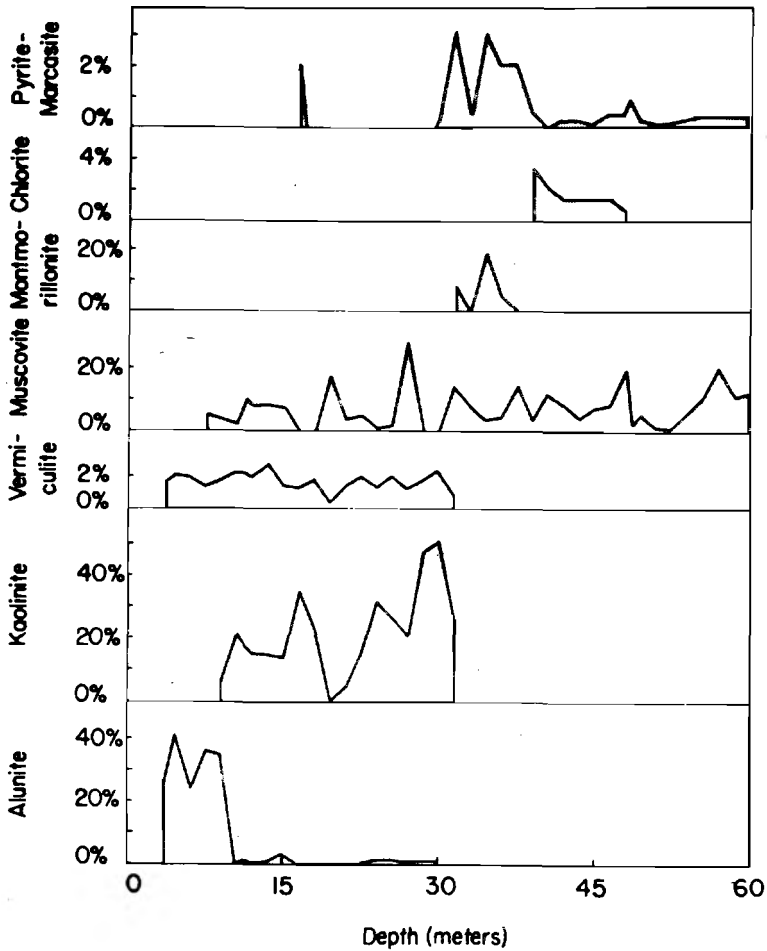


FIG. 4. Abundance of major alteration minerals in DDH 76-1, in weight percent.

←

FIG. 3. Bulk rock (solid symbols) and glass (open symbols) normative compositions plotted in the system albite-orthoclase-quartz. Squares are Quaternary rhyolite, triangles are Tertiary rhyolite of Corral Canyon. The curved line represents the quartz-alkali feldspar boundary at 500 bar water pressure. Feldspar compositions in volcanic rocks are shown in the lower triangle. Phenocrysts are solid circles, groundmass are open circles, and crosses represent feldspars from Tertiary rhyolite from Corral Canyon. Coexisting feldspars from rhyolite domes are shown by tie lines. Rock and mineral analytical data are tabulated by Evans and Nash (1978).

altered quartz monzonite. Very fine-grained alunite and opal replace all but quartz grains in alluvium from the granite. Opal fills and lines fractures and intergranular pore spaces. Opal-rich zones contain traces of realgar and up to 5 percent native sulfur. Kaolinite first appears at 9 to 18 m, montmorillonite at 20 to 35 m, and K-mica at 6 to 32 m. Jarosite occasionally fills intergranular pore spaces and fractures along with traces of barite. Pyrite with marcasite overgrowths are present below the water table at about 32 m. Altered and brecciated gneiss contains varying proportions of bleached, sericitized biotite, K-feldspar, plagioclase, pyrite, marcasite, kaolinite, K-mica, and montmorillonite. Hydrothermal K-feldspar partially replaces a few plagioclase crystals and fills fractures.

Vermiculite, muscovite, clay, and calcite replace biotite in altered quartz monzonite (Figure 4) in

Table 3. Chemical\* and modal analyses of rocks from the Roosevelt Hot Springs thermal area.

Sample no. description	R9 sinter	R3 sinter cemented alluvium	DDH 76-1, 4.6 m sinter cemented acid sulfate altered alluvium	DDH 76-1, 22.9 m argillized quartz monzonite	DDH 76-1, 47.3 m weakly propylitized quartz monzonite
SiO <sub>2</sub>	91.8	85.9	55.1	76.0	65.6
Al <sub>2</sub> O <sub>3</sub>	2.6	4.7	17.9	13.9	17.1
TiO <sub>2</sub>	0.00	0.08	0.36	0.58	0.71
Fe <sub>2</sub> O <sub>3</sub> †	0.82	1.0	0.98	0.44	3.
MgO	0.10	0.29	0.37	0.37	0.86
CaO	0.11	0.45	0.34	0.33	1.7
Na <sub>2</sub> O	0.10	1.2	n.d.	n.d.	4.0
K <sub>2</sub> O	0.09	1.6	3.9	3.8	6.4
L.O.I.‡	3.48	3.40	6.60	4.20	0.88
SO <sub>3</sub>	0.15	0.07	14.2	0.51	
S					0.15
S = O					0.08
Total	99.3	98.7	99.8	100.1	100.5
Modal composition in weight percent					
Quartz	94	74	54	48	16
Plagioclase An <sub>10</sub>	2	12		3	37
K-feldspar	.1	10		23	29
Biotite	.7	2			5
Muscovite				5	10
Alunite	.5	.2	41	0.6	
Kaolinite				16	
Vermiculite			2	2	
Chlorite					1
Pyrite					0.4
Sphene	.2	.3			
Rutile			.4	0.5	0.7
Hematite	.7	.7			

\* XRF analysis using the method of Norrish and Hutton (1969).

† Total iron as Fe<sub>2</sub>O<sub>3</sub>.‡ Loss on ignition less SO<sub>3</sub>.

Table 4. Selected Roosevelt Hot Springs water analyses in mg per liter.

	Sample 1	Sample 2	Sample 3	Sample 4
Na	1840	1800	2072	2500
Ca	122	107	31	22
K	274	280	403	488
SiO <sub>2</sub>	173	107	639	313
Mg	25	24	.26	0
Cl	3210	3200	3532	4240
SO <sub>4</sub>	120	70	48	73
HCO <sub>3</sub>	298	300	25	156
Al			1.86	.04
Fe			.016	
Total dissolved solids	6063	5888	6752	7792
Temperature	25°C	28°C	92°C	55°C
pH	6.5	6.43	5.0	7.9
Na-K-Ca Temperature	241°C	239°C	274°C	283°C
SiO <sub>2</sub> Temperature	170°C	140°C	283°C	213°C

Sample (1), Roosevelt Seep, University of Utah, June, 1975. Sample (2), Roosevelt Seep, Phillips Petroleum Co., August, 1975. Sample (3), Thermal Power Co. well 72-16, Univ. of Utah, Jan., 1977. Surface leakage. Sample (4), Roosevelt Hot Springs, Sept., 1957, U.S.G.S., Mundorff (1970).

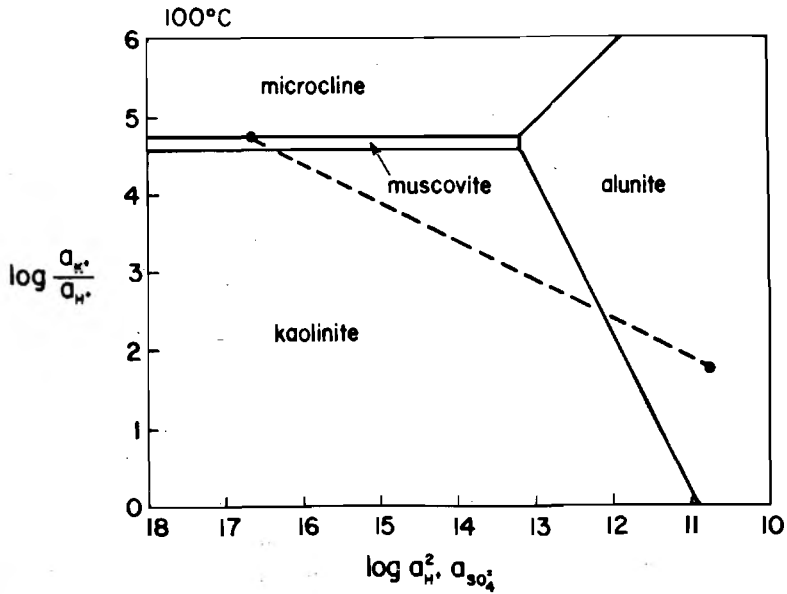


FIG. 5. Activity diagram of the system  $K_2O-Al_2O_3-SiO_2-SO_3-H_2O$  at  $100^\circ C$  and quartz saturation showing one calculated reaction path for microcline and Roosevelt thermal water.

DDH 76-1. Feldspars are replaced by clay, muscovite, calcite, opal, and chalcedony. Veinlets of pyrite, green muscovite, opal, and chalcedony are common. Thin veinlets of K-feldspar-quartz intergrowths are present from 49 to 61 m. Chemical and modal analyses of altered rocks are shown in Table 3, and abundances of alteration minerals in one shallow core hole (76-1) are shown in Figure 4.

Hydrothermal alteration is closely associated with fractures in the Mineral Mountains pluton to a depth of 2 km in Thermal Power Co. well Utah State 14-2 (Figure 2). Clay minerals montmorillonite and mixed layer clays, commonly found only near the surface near the Opal Mound fault, occur to a depth of 500 m in well 14-2 with K-mica, K-feldspar, pyrite, calcite, and limonite. The deeper alteration assemblage from 500 m to 2 km consists of K-mica, chlorite, calcite, K-feldspar, and pyrite.

Anomalous concentrations of mercury, arsenic, and lead are associated with the altered rocks. Mercury anomalies as high as 3 ppm are localized over faults in surface rocks. Maximum arsenic in surface rocks is 2000 ppm near the opal mound, and 430 ppm in altered rocks in drill holes. Maximum lead content of altered rocks is 400 ppm in altered alluvium in one drill hole.

Computational methods of Helgeson (1968) were

used in a simplified thermodynamic model of the alteration, in which starting materials consist of microcline and a solution similar to the Roosevelt Hot Springs reservoir water. Thermodynamic data used are those of Helgeson (1969) and Hemley et al (1969). In the model, the dominant reaction process is an exchange of potassium from microcline for hydrogen from solution (Figure 5). The quantity of microcline consumed per kilogram of solution is a function of temperature and solution pH. Alteration zoning is a function of thermal and pH gradients.

A plausible hypothesis that has been developed for the Steamboat Springs, Nevada thermal system (Schoen et al. 1974) is also applicable for the development of the surface and near-surface alteration at the Roosevelt Hot Springs thermal area. Hot aqueous solutions in equilibrium with K-feldspar, chlorite, muscovite and quartz, containing  $H_2S$  and sulfate convectively rise along major fractures. At the surface,  $H_2S$  oxidizes to sulfate decreasing pH and causing alunite to form. Cooling causes opal to precipitate. Low pH, high sulfate, surface water flows away from the fracture and percolates downward. As alunite continues to form, hydrogen ion and sulfate are consumed and kaolinite precipitates as shown in Figure 5. Stability fields for muscovite and K-feldspar are encountered downward.

### Water chemistry

Chemical analyses of surface and deep thermal waters are summarized in Table 4. While there is some variability, the analyses indicate that the thermal waters are relatively dilute (ionic strength = .1 to .2) sodium-chloride brines. Sulfate concentrations vary between 48 and 120 mg/l and total dissolved solids are approximately 7000 mg/l. Chemical differences exist between surface and deep thermal fluid, consisting principally of higher  $Mg^{++}$ ,  $Ca^{++}$ , and  $SO_4^-$  and lower Na, K, and  $SiO_2$  in surface relative to deep waters. These differences presumably reflect progressive leaching of Mg and Ca by ascending thermal fluids, oxidation of  $H_2S$  or admixture of oxidized,  $SO_4^-$  rich, surface waters, and flashing and cooling with subsequent precipitation of opal. The Roosevelt Hot Springs thermal fluids are hot-water dominated, in the terminology of White (1970). Thus, the Roosevelt Hot Springs geothermal fluids are chemically similar to New Zealand geothermal fluids.

White (1957) described waters that are variously enriched with sodium chloride,  $H^+$ , sulfate, and biocarbonate. Within White's definitions, Roosevelt Hot Springs water could be defined as a sodium chloride water grading into an acid sulfate water. The sulfate measurements of 48–120 mg/l (at Roosevelt Hot Springs) are lower than those at Norris Basin, Yellowstone Park (454 ppm), or Frying Pan Lake, New Zealand (262 ppm) which have been defined as acid-sulfate, chloride waters. Both Na and Cl contents of waters from Roosevelt Hot Springs are considerably higher than for sodium chloride waters described by White (Steamboat Springs, Washoe County, Nevada; Morgan Spring, Tehama County, California; Norris Basin, Yellowstone Park, Wyoming; Well 4 Wairakei, New Zealand).

Application of the Na-K-Ca and  $SiO_2$  thermometers (Fournier and Truesdell, 1974) to the seep and the deep geothermal fluid indicates deep water temperatures of 241° and 286°C, respectively, which agree well with deep down-hole measurements. The Na-K-Ca wall-rock equilibration temperature on the Roosevelt seep sample is one of the highest calculated subsurface temperatures in Utah. This high temperature and the presence of extensive surface opal deposits first suggested a viable geothermal resource at Roosevelt Hot Springs.

### GEOPHYSICS

Numerous geophysical techniques used at the Roosevelt Hot Springs thermal area have aided understanding of the convective hydrothermal system, but no one method has been capable of pro-

viding unequivocal targets for drilling, nor has the collection of methods unequivocally located the source of heat. Nevertheless, when combined with geologic and geochemical data, the sum of the geophysical data sets materially assists in limiting the drilling target. Microearthquakes and gravity and magnetic surveys have been used to define the regional setting and the faulting; resistivity, electromagnetic and heat flow surveys have been used to localize the convective hydrothermal system; while magnetotelluric, gravity, magnetic, and refraction seismic surveys, and  $P$ -wave delay times have been used in attempts to locate the source of heat. Multiple data set modeling, now in progress, is expected to contribute significantly to the objectives of this research.

### Microearthquakes

Regional seismicity has shown that the Roosevelt Hot Springs and Cove Fort areas are located where the north-trending intermountain seismic belt (Smith and Sbar, 1974) intersects the Pioche-Beaver-Tushar mineral trend (Stokes, 1968). This latter trend is a significant tectonic feature because it cross-cuts the north-trending Late Cenozoic horsts and grabens of the eastern Great Basin. It is seismically active (Eaton, 1978) and may reflect a highly fractured crust that could facilitate magma migration into the upper crust and thus enhance the geothermal potential.

In 1974 and 1975, earthquake monitoring of both the Roosevelt Hot Springs and Cove Fort areas was conducted as a means of examining the relationships between seismicity and the known geothermal features (Olson and Smith, 1976). The surveys used up to 12 portable, high-gain seismographs (see Figure 6 for station locations). In 49 days of monitoring, 163 earthquakes of magnitude  $-0.5 < M_L < 2.8$  were located. Numerous small earthquakes scattered about an area 6 km north of Cove Fort were not locatable because they were not recorded at a sufficient number of stations. The seismic activity was characterized by shallow-focus earthquakes, most less than 10 km deep. The earthquakes were grouped in three areas: (1) a north-south trend of moderate activity on the west side of Milford Valley; (2) a trend of minor activity along the west side of the Mineral Mountains, including the Roosevelt Hot Springs thermal area; and (3) an area of numerous swarm-like earthquake sequences around the Cove Fort area. These earthquake data suggest that the Roosevelt Hot Springs thermal area is only slightly active and at a much lower level than the earthquake zones 60 km east near Richfield and Marysvale, Utah.

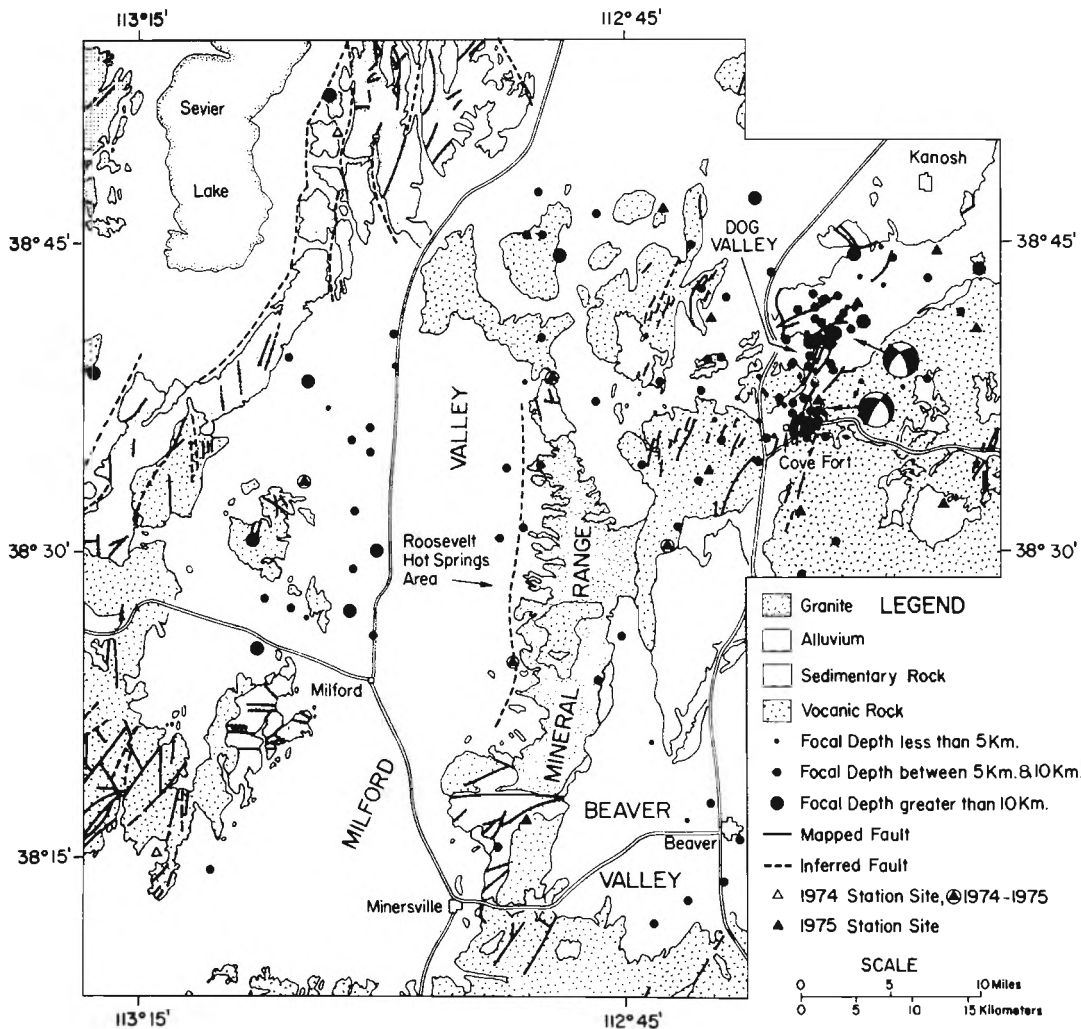


FIG. 6. Epicenter map of the Roosevelt Hot Springs-Cove Fort, Utah area from earthquake surveys in 1974 and 1975. Fault plane solutions are lower-hemisphere, equal-area stereographic nets. Dark areas are quadrants of compression; light areas are quadrants of dilatation. Arrows indicate directions of minimum compressive stress ( $T$ -axes).

$P$ -wave traveltimes, as measured across three stations on the west flank of the Mineral Mountains (Figure 6) from earthquakes 30 km away near Cove Fort, showed slight positive delays (later arrivals) of up to 0.2 sec. These delays could have been produced from lateral velocity variations or near-surface low-velocity material which were not defined. Alternatively, they could have been produced by an upper crustal low-velocity layer beneath the Mineral Mountains. The resolution was not sufficient to delineate the layer.

$S$ -wave delays could not be calculated. However, qualitative estimates of  $S$ -wave attenuation at a station south of Roosevelt Hot Springs, from the Cove Fort earthquake sources, suggest a low- $Q$  transmission path. Thus, the raypaths that propagate beneath the Mineral Mountains showed both a low-velocity effect and shear wave attenuation possibly indicative of partial melting or of major intense fracturing of the intersected crustal rocks beneath the southern part of the Mineral Mountains.

Fault-plane solutions (Figure 6) for the Cove Fort

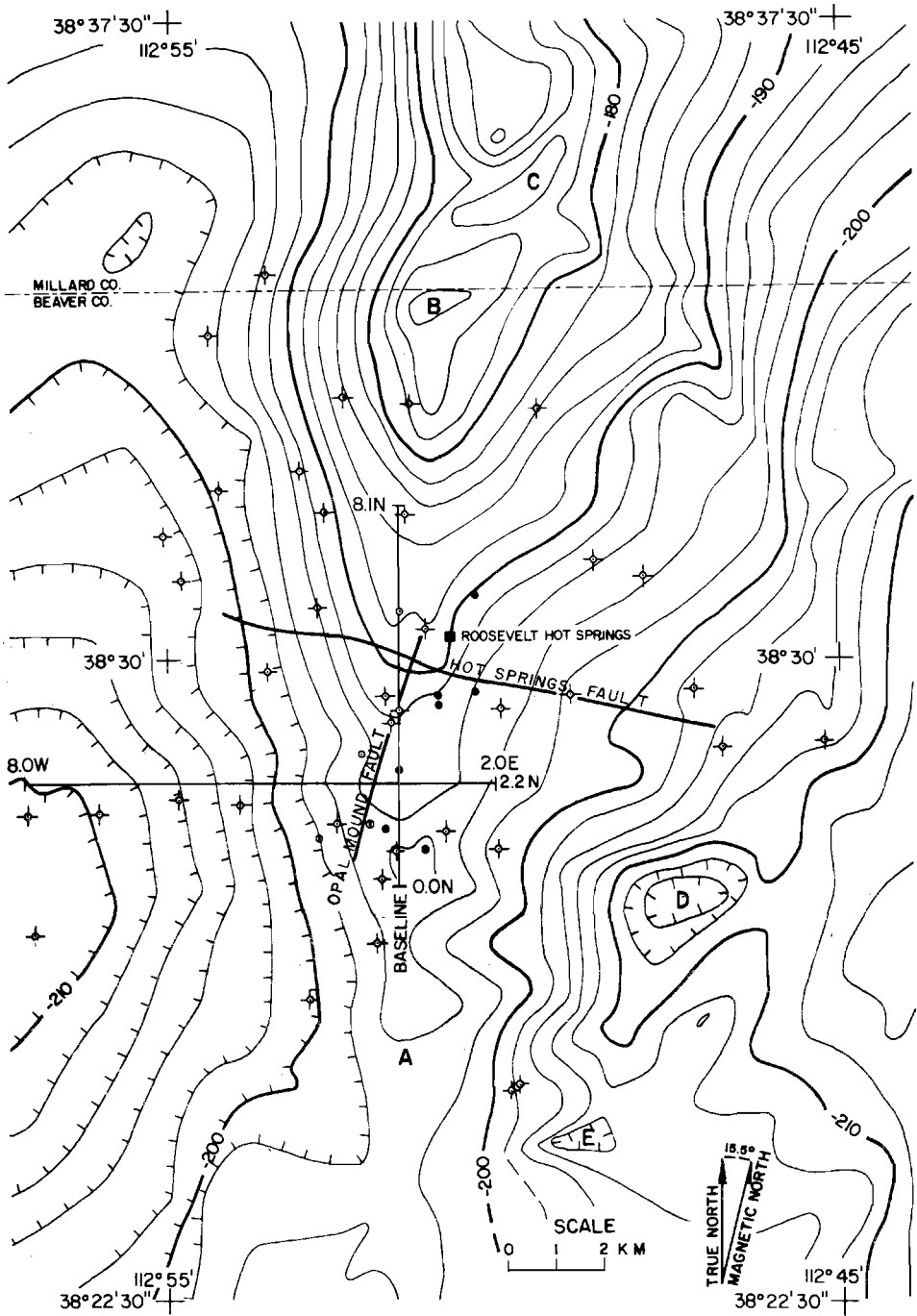


FIG. 7. Terrain-corrected Bouguer gravity anomaly map of the Roosevelt Hot Springs thermal area. Contour interval = 2 mgal. Well designations: solid circle, productive well; plain open circle, nonproductive well; open circle, with crosses, thermal gradient well. Letter designations are described in text.

earthquakes demonstrate oblique normal faulting with west to west-northwest directions of the minimum compressive stress. This stress direction is consistent with general east-west extension of the eastern Great Basin. Such east-west extension could have allowed development of conduits through which thermal fluids have traveled upward to reach the Roosevelt Hot Springs thermal area.

The nature of earthquake occurrence at Cove Fort was unusually episodic and demonstrated swarm-type characteristics. A maximum likelihood estimate of  $b$ -values at Cove Fort was  $0.84 \pm 0.16$ , but values as large as  $1.27 \pm 0.18$  were calculated for the intense swarm activity at Dog Valley. Earthquakes that occur in volcanic and ocean-spreading settings usually have  $b$ -values of 1.0 or greater. Thus the argument for a volcanic relationship of the Cove Fort seismicity can be made. However, the degree of complex faulting at the intersection of two tectonic trends argues for a locally complex stress field that could produce swarm-type earthquakes and unusually high  $b$ -values.

Statistical modeling of the Cove Fort earthquake swarms showed a symmetrical distribution of probabilistic estimates of energy levels. It also showed the general increase in the probability of earthquake occurrence versus energy. These results are similar to those of a published oceanic earthquake swarm (Sykes, 1970). This does not imply a causal relationship, but the statistical modeling and the close spatial association of the Cove Fort-Dog Valley earthquake swarms with the nearby Quaternary basalts suggests that the potential exists for a geothermal source related to Holocene volcanism.

### Gravity and magnetic surveys

Figure 7 shows the terrain-corrected Bouguer gravity anomaly map based on about 700 stations occupied during 1974 through 1976. The generally northward-trending gravity contours, with pronounced gradients over the alluvium adjacent to the western margin of the Mineral Mountains, indicate that the mountains are bounded on the west by basin and range faults; these faults form the eastern margin of the Milford Valley graben, which is reflected in the gravity low along the western part of the map. Two northward-trending, elongate gravity highs, which are right-laterally offset about 2 km in the intervening area of a large gravity saddle in the Ranch Canyon area (A of Figure 7), extend throughout the central part of Figure 7. The northern gravity high overlies principally the western margin of the Mineral Mountains where granitic rocks are exposed; and the elongate gravity spur extending southward from the

southern peak of the high (B in Figure 7) corresponds in a striking manner, both in trend and areal extent, with the pronounced heat flow anomaly (Figure 14) related to the known geothermal reservoir (Crebs and Cook, 1976; Carter and Cook, 1978). Where the Hot Springs fault (shown in Figures 2 and 7) intersects the spur, the regularity of the contours is significantly disrupted. The southern gravity high, which extends off the map to the south, overlies the southern part of the Mineral Mountains where undated metamorphic and Paleozoic sedimentary rocks occur (Thangsuphanich, 1976). About 2 km north of the Millard-Beaver county line, a fault zone (herein designated the "county line fault") occurs (C of Figure 7; also shown on Figure 2) where the Mineral Mountains pluton terminates against Paleozoic rocks, and the northern gravity high is separated into two separate gravity highs which are right-laterally offset about 2 km in the intervening area of a gravity saddle. In the southern part of the gravity map is a pronounced north-northeastward-trending elongate gravity feature, about 8 km in length and consisting of two gravity lows (D and E of Figure 7). This gravity feature corresponds with a series of rhyolite domes, including Bearskin and Little Bearskin Mountains, and North and South Twin Flat Mountains, and possibly indicates a low-density continuous intrusive body at shallow depth (2 km) beneath the rhyolite domes (Crebs and Cook, 1976; Carter and Cook, 1978).

Figure 8 shows a total magnetic intensity residual anomaly map. The broad northward-trending magnetic high, of about 250 gammas of average total relief, that extends throughout the central part of the map, corresponds with the Mineral Mountains granitic pluton. The small magnetic highs correspond with local areas of increased magnetic susceptibility of both the granitic-type rocks within the pluton and the metamorphic rocks that are found both exposed and in drill holes principally along the western margin of the range south of the Hot Springs fault. In the south-central part of the map, the striking constriction of the magnetic high anomaly corresponds with (1) a similar constriction of the exposed pluton as a consequence of the previously mentioned volcanic domes which intrude the pluton in this area, (2) a postulated east-west structural lineament in this area, and (3) the southern end of the pronounced heat flow anomaly (Figure 14). Near the northern edge of the map (F of Figure 8), the striking east-west linear trend of the magnetic contours, with a large gradient, corresponds with the northern margin of the Mineral Mountains pluton and the county line fault (shown



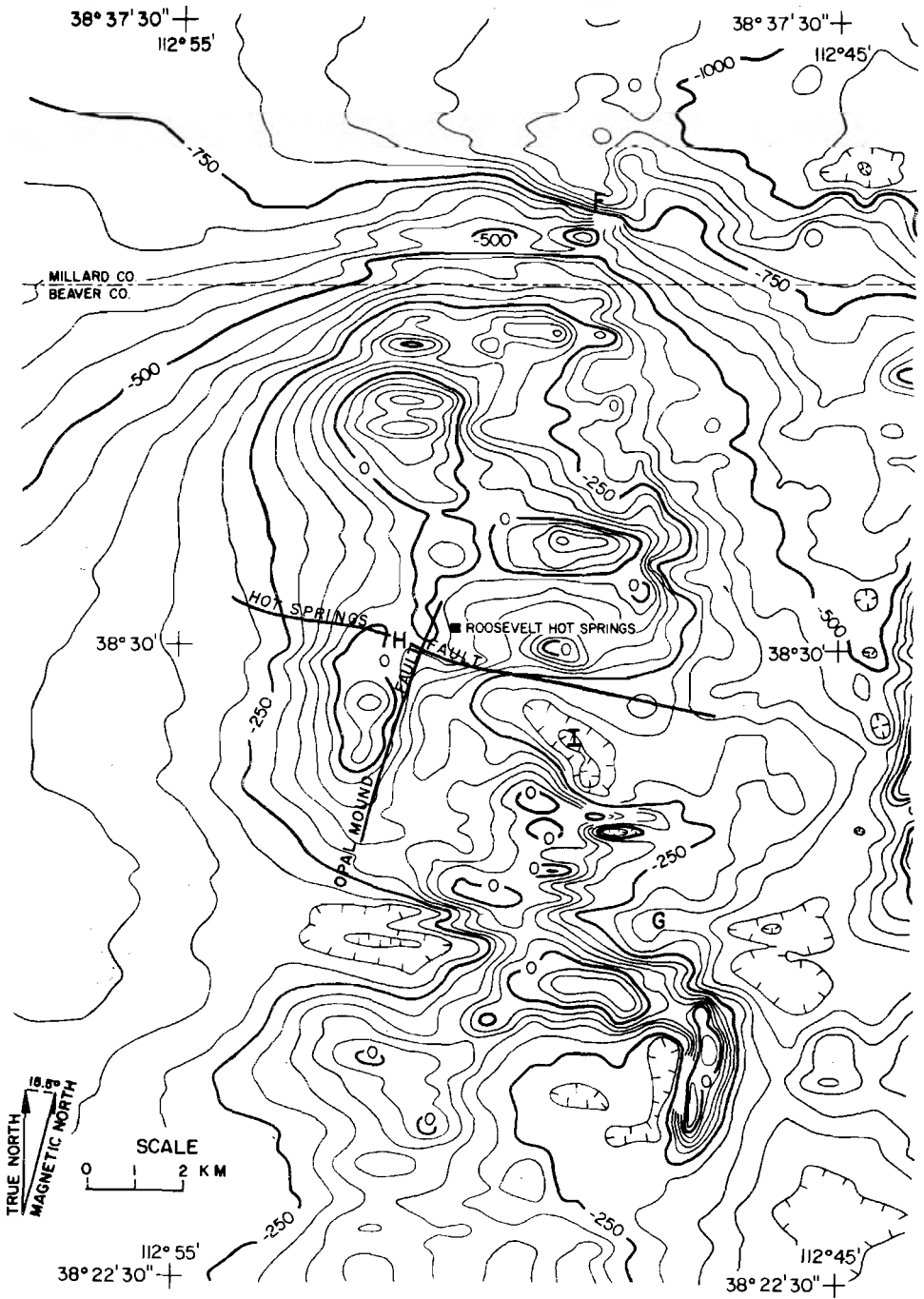


FIG. 8. Total aeromagnetic intensity residual anomaly map of the Roosevelt Hot Springs thermal area. Contour interval = 50 gammas. Data were obtained along east-west lines at 1/4-mile (402-m) spacing, drupe flown at an elevation of 1000 ft (305 m) above ground. International Geophysical Reference Field (IGRF), updated to 1975, is removed from data. Letter designations are described in text.

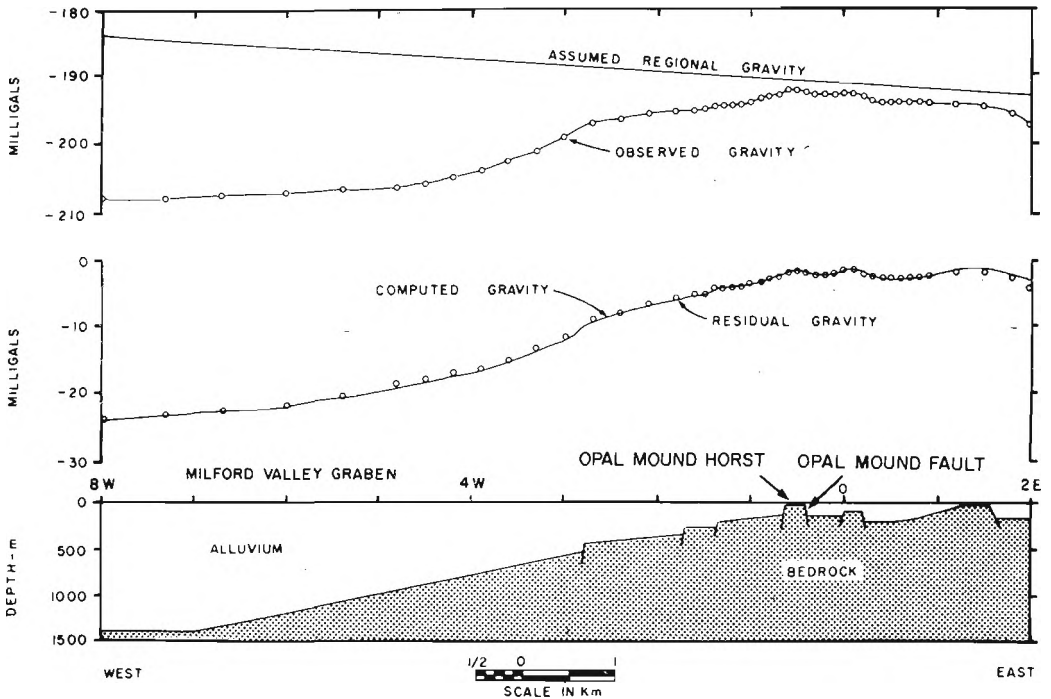


Fig. 9. Interpretative two-dimensional model for gravity profile along line 2.2N (see Figure 7) of the Roosevelt Hot Springs thermal area. Assumed density contrast is  $0.5 \text{ g/cm}^3$ .

in Figure 2). The westward continuation of the lineament across Milford Valley indicates that the high magnetic susceptibility material (probably granitic) may extend under the alluvium of Milford Valley. The magnetic and gravity data (Brumbaugh and Cook, 1977) indicate that this pervasive east-west structural lineament extends eastward to the Cove Fort area (Figure 6) and beyond.

Other magnetic features which correlate well with the geology and/or gravity features are: (1) a magnetic low (G of Figure 8) which partly overlies the previously mentioned Bearskin and Little Bearskin volcanic domes; (2) an east-west magnetic lineament along the Hot Springs Fault (H of Figure 8) with a 2-km right-lateral offset of magnetic highs on opposite sides of the fault near the western margin of the Mineral Mountains; and (3) a magnetic low that corresponds almost exactly in areal extent with the reversed magnetic polarity of the Bailey Ridge rhyolite flow (I of Figure 8).

Figures 9 and 10 show the terrain-corrected Bouguer gravity anomalies and interpretative geologic cross-sections along the east-west line 2.2N and the north-south baseline, respectively (Crebs and

Cook, 1976). Both lines cross the area of high heat flow (Figure 14). For these models, the density contrast between the bedrock and alluvium is assumed to be  $0.5 \text{ g/cm}^3$ . The gravity data on line 2.2N (Figure 9) indicate: (1) the northward-trending Opal Mound horst, which is bounded on the east by the geologically mapped Opal Mound fault with an indicated vertical displacement of about 50 m; (2) step faults in the bedrock bounding the eastern margin of the Milford Valley graben; and (3) an alluvium thickness of about 1.4 km beneath Milford Valley at the western end of the profile. The gravity data on the baseline (Figure 10) indicate: (1) the eastward-striking Hot Springs Fault, downthrown on the south, with a vertical displacement of about 65 m; and (2) another eastward-striking fault at 6.5N, downthrown on the north, with a vertical displacement of about 60 m. These two models, based on gravity data, indicate that many pronounced faults, striking both north-south and east-west, occur in the Roosevelt Hot Springs thermal area. Although the area lying east of the Opal Mound fault and west of the granite outcrop is modeled along line 2.2N (Figure 9) with only two faults, the gravity data do not pre-

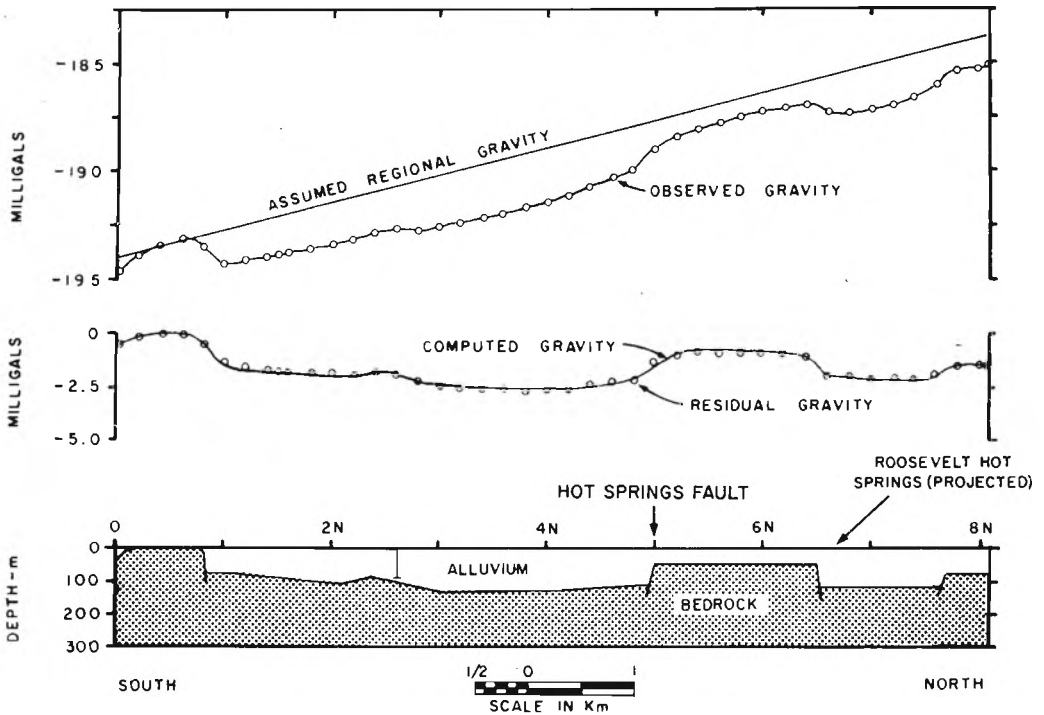


FIG. 10. Interpretative two-dimensional model for gravity profile along baseline (see Figure 7) of the Roosevelt Hot Springs thermal area. Assumed density contrast is  $0.5 \text{ g/cm}^3$ .

additional faulting and fracturing in this area.

In the Ranch Canyon area (A in Figure 7), the large gravity saddle and the roughly corresponding magnetic saddle are possible expressions of a deeply buried intrusive body of low density and low-magnetic susceptibility. However, the gravity saddle may be caused by the combined effects of (1) the overlap of the gravity lows associated with the Milford Valley and Beaver Valley grabens on the west and east sides, respectively, of the Mineral Mountains; and (2) the near-surface silicic volcanics (Carter and Cook, 1978). At present, therefore, it cannot be concluded that the gravity and magnetic saddles are caused by a partial melt of low density and low-magnetic susceptibility under the Mineral Mountains.

### Electrical measurements

Electrical surveys performed in the Roosevelt Hot Springs thermal area include 100-m, 300-m, and 1-km dipole-dipole resistivity, Schlumberger resistivity, electromagnetic, and magnetotelluric soundings. The amount of data so recorded has provided an insight into the three-dimensional geoelectric section. For example, Figure 12 (after Ward and Sill, 1976b)

portrays the contours of apparent resistivity observed over the geothermal field in first separation 300-m dipole-dipole resistivity surveying. It represents, we believe, the distribution of brine-soaked montmorillonite and mixed-layer clays in the top 500 m of the system; this opinion is based on the alteration studies described earlier. The clays are alteration products of feldspars and occur dominantly along faults and fractures (Figure 11) in the Tertiary granite host rock. Surface conduction in the kaolinite and montmorillonite secondary clay minerals is estimated to be three times as important as conduction via the high temperature brine existing in the fractures (Ward and Sill, 1976a).

Insofar as clay alteration is most dominant along fractures, it is not surprising that the 100-m dipole-dipole survey delineated most of the major fractures of the geothermal field. Figure 11 depicts fractures interpreted from aerial photography (*P*), observed geology (*G*), dipole-dipole resistivity surveys (*R*), and aeromagnetic surveys (*M*). The density of inferred fractures or faults is greatest where data density is greatest and that occurs in the vicinity of the Opal Mound fault. Three fracture sets, trending north-

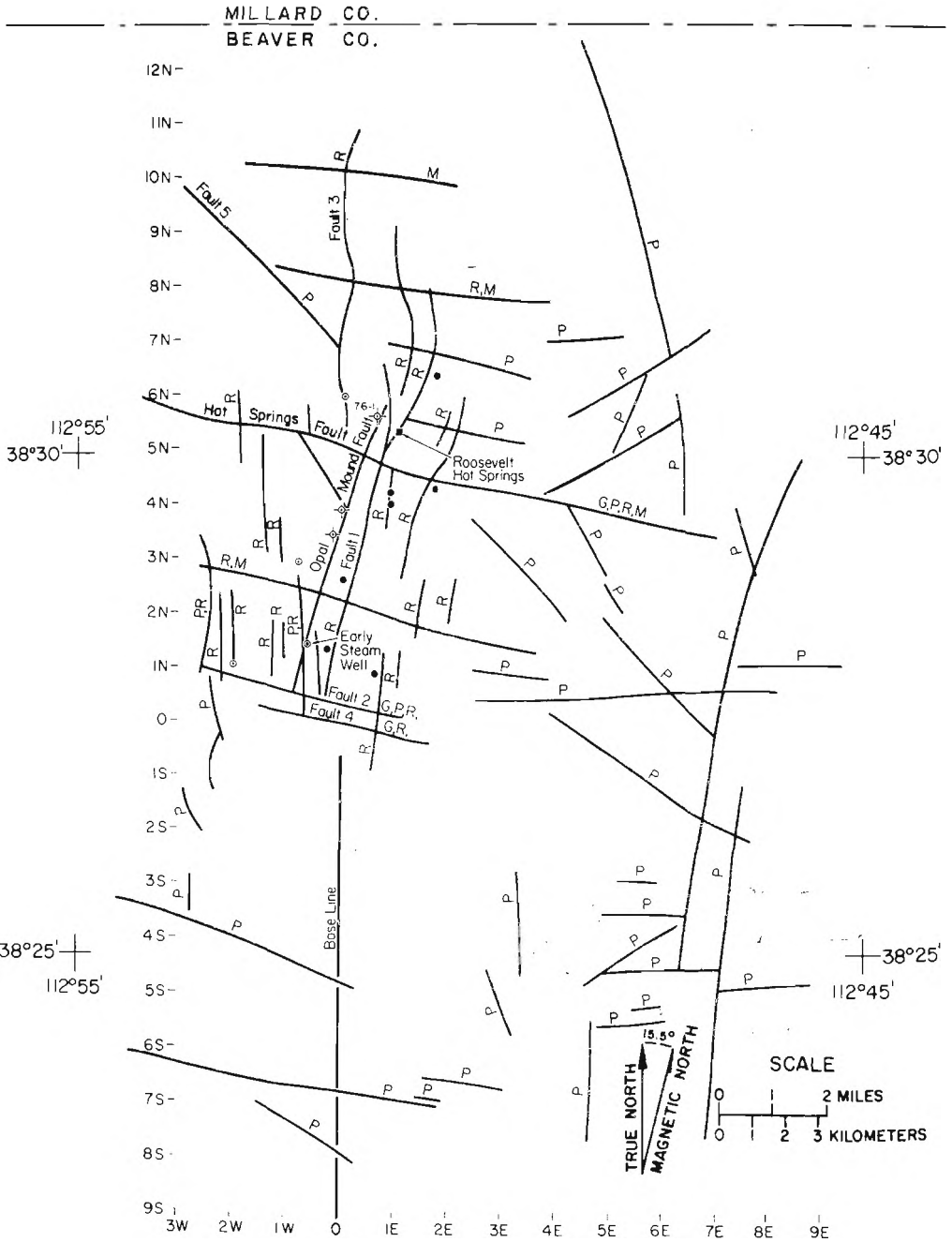


FIG. 11. Lineaments, interpreted as fractures and faults, mapped by photos (*P*), geologic observation (*G*), resistivity survey (*R*), and aeromagnetic survey (*M*) over the Roosevelt Hot Springs thermal area. Producing wells shown by solid dots, "dry wells" by open circles, shallow alteration holes by circles with crosses.

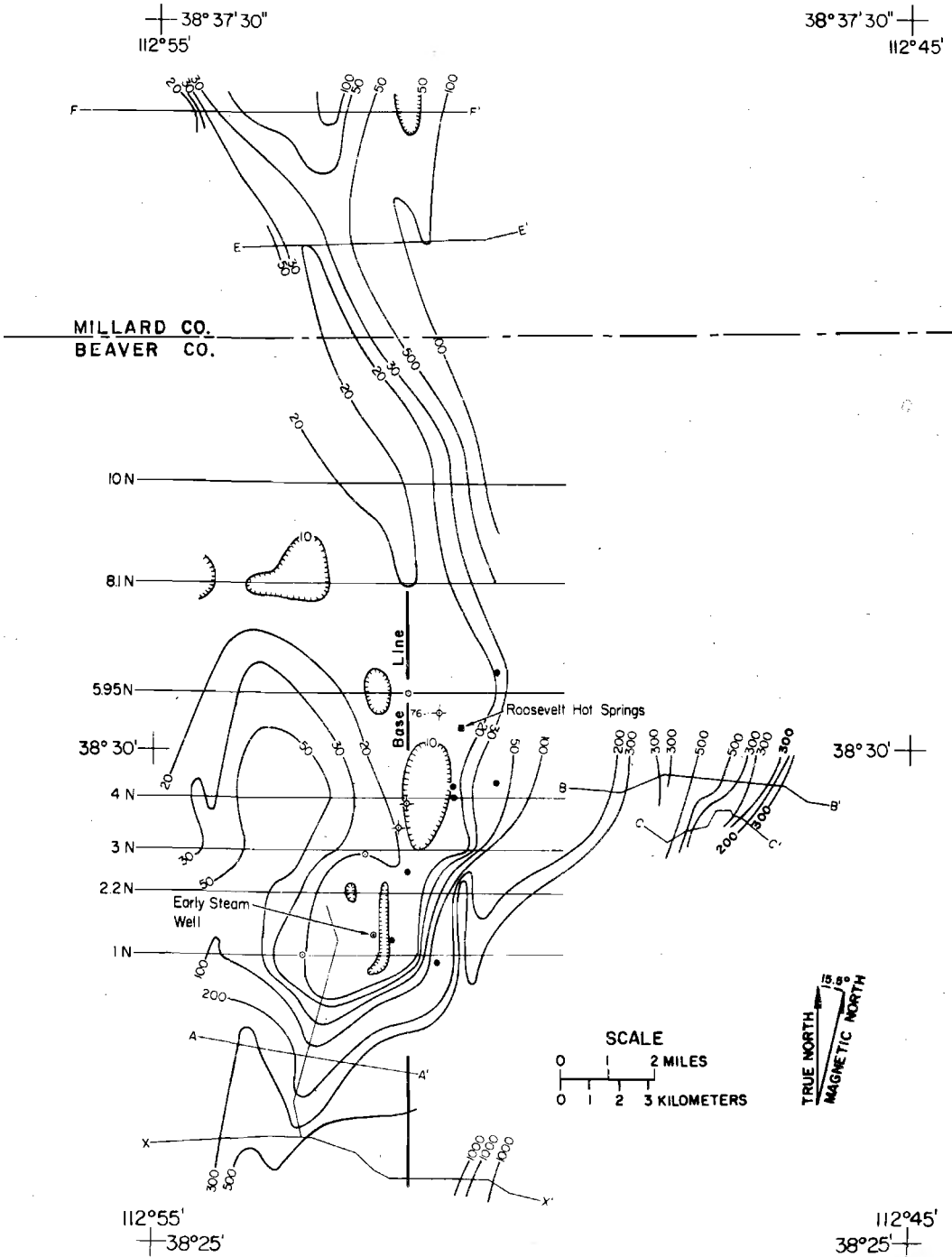


FIG. 12. Contours of apparent resistivity obtained with dipole-dipole array, first separation, over the Roosevelt Hot Springs thermal area. Contours at 10, 20, 30, 50, 100 Ω-m and multiples of ten times these figures. Productive wells shown by solid dots, "dry wells" by open circles, shallow alteration holes by circles with crosses. Traverse lines are shown.

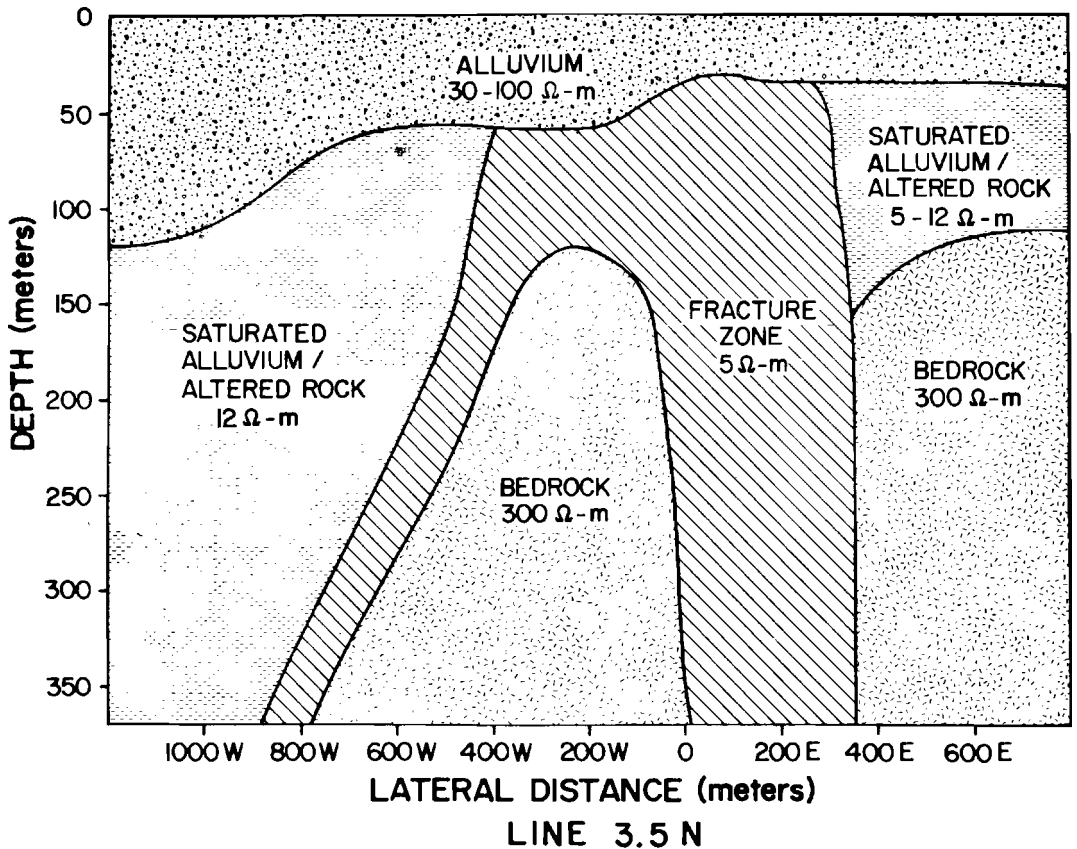


FIG. 13. Pseudo-geologic interpretation of geoelectric section obtained from several electrical surveys along traverse 3.5N (see Figure 12 for coordinate location) of the Roosevelt Hot Springs thermal area.

northeast, west-northwest, and northwest are in evidence. Further, the granitic terrain is highly fractured leading us to explain the high permeability of the reservoir as fracture-dominated.

The northwest-southeast and east-west fractures probably provide conduits for meteoric water recharge of the reservoir to the east of the Opal Mound fault and probably provide conduits for westward leakage of geothermal brine to the Milford Valley (Ward and Sill, 1976a). Resistivities beneath the first 30 to 100 m of alluvium in the valley range from 2  $\Omega$ -m down to 0.1  $\Omega$ -m suggesting brine-saturated alluvium and/or saline Lake Bonneville sediments.

Tripp et al (1978) summarize the contributions of the Schlumberger and electromagnetic data as follows:

One- and two-dimensional modeling of the Schlumberger soundings at the Roosevelt Hot Springs KGRA have indicated a low-resistivity

zone of approximately 5  $\Omega$ -m paralleling the Dome fault. The low resistivity of this zone is probably due to intensely fractured and altered water-saturated rock. A zone of resistivity 12  $\Omega$ -m extending to the west of the Opal Mound fault is probably due to leakage of brine away from the geothermal system through alluvium or moderately altered rock. A resistive basement underlies the conductive zones and is believed to be relatively nonporous and unaltered rock.

A major problem in the application of 1-D modeling of Schlumberger data in the Roosevelt Hot Springs KGRA is poor resolution of the 1-D model parameters. The joint inversion of Schlumberger and EM sounding data gives a least-squares 1-D conductivity model in which parameters are much better resolved than the model parameters estimated by the inversion of Schlumberger data alone.

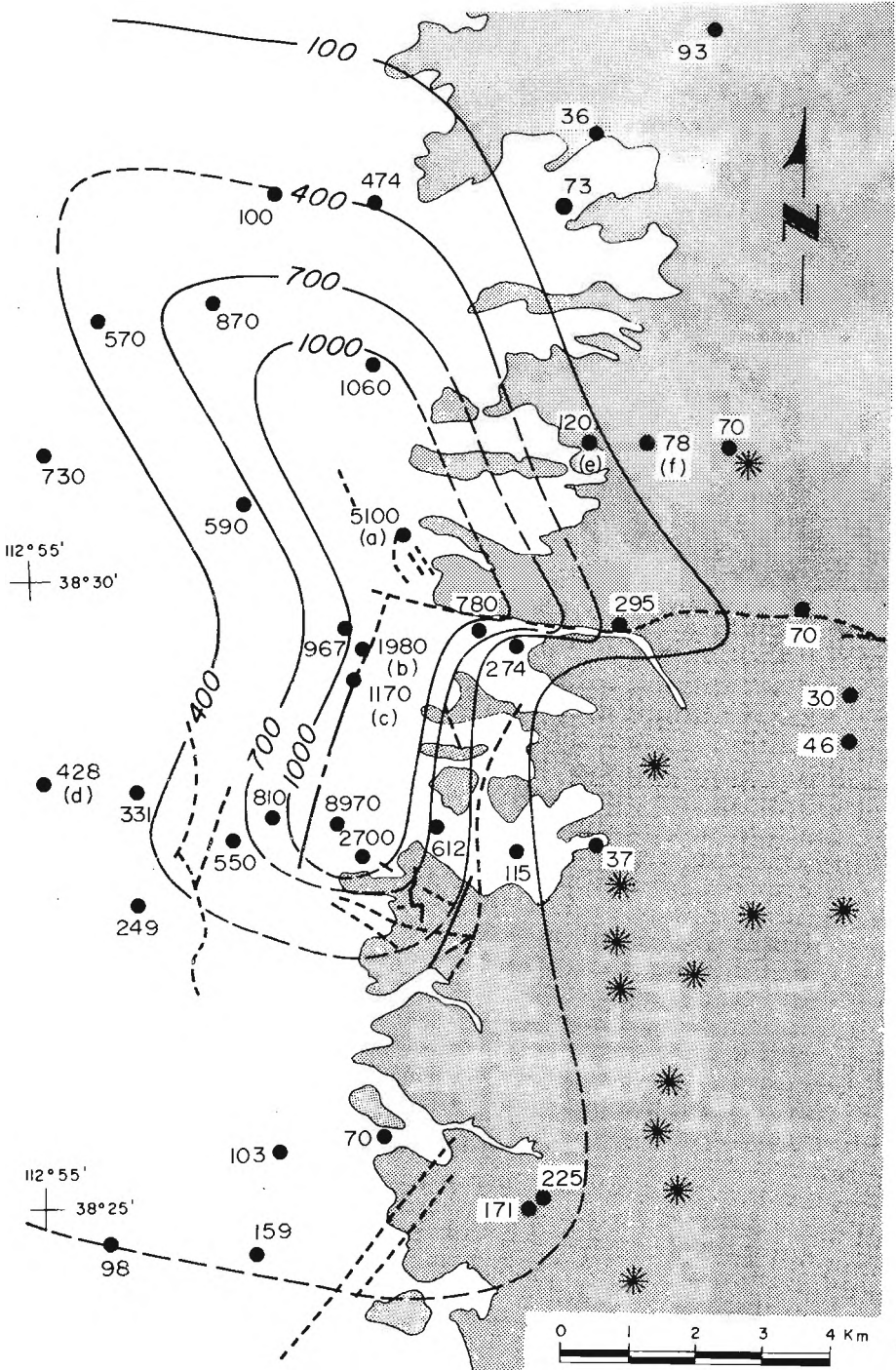


FIG. 14. Heat flow map of the Roosevelt Hot Springs geothermal area. Solid dots and adjacent numbers indicate sites and heat flow values in  $\text{mW m}^{-2}$ . The outcrop pattern of the 10 m.y.-old Mineral Mts. pluton is shaded with the vents for the younger flows (0.8 m.y.), and rhyolite domes (0.5 m.y.) indicated by asterisks. Major fault patterns are indicated by heavy solid and broken lines.

One-dimensional modeling of Schlumberger soundings along a traverse does indicate the presence of a 2-D inhomogeneity, but it gives no hint of the possible complexity of that inhomogeneity even though the parameters of the models fitting each sounding have acceptable standard deviations when constrained by EM sounding data. Since the model parameter standard deviations are model dependent, good resolution of 1-D model parameters does not indicate that the assumption of a 1-D model is valid. On the other hand, the possible complexity of structure is brought out by 2-D modeling of the same data, but since the number of degrees of freedom for complex 2-D models is large, a thorough study of the resolution of such models is prohibitively costly at present. In these circumstances, we must constrain the 2-D models with independent geologic or geophysical data and then accept the subsequent best-fit model as semiquantitative.

When we combine all of the data from the active electrical methods we readily generate the pseudo-geologic model of Figure 13. This figure is based on a subjective combination of 1-D inverse interpretations of combined Schlumberger and EM soundings, and 2-D forward interpretations of both Schlumberger and dipole-dipole data using geologic, geochemical, and other geophysical constraints. It is our best model to depths of 500 m for line 3.5N of Figure 12, beyond which the active electrical methods totally lack resolution in this environment as established by sensitivity tests (Ward and Sill, 1976a).

The apparent resistivities from 85 magnetotelluric and audio-magnetotelluric (MT/AMT) soundings have been inverted to 1-D model earths at each sounding site. We believe that the resulting models are totally unrealistic representations of a subsurface distribution of true resistivities (Wannamaker et al, 1978). The interpreted resistivities of less than 0.1  $\Omega$ -m at depths of 2 to 5 km are virtually impossible to obtain unless graphitic horizons or massive sulfides are present, given that our earlier discussion indicated that clay alteration should be absent at these depths. Insofar as our current geologic evidence precludes graphite or sulfides, we are inclined to believe that the resistivities in the 2 to 5 km range interpreted from the MT/AMT data are artifacts of the interpretation technique and could readily arise in conductive materials in the top 0.5 km. That the conventional means of identifying TE and TM modes is inapplicable in this 3-D resistivity environment also arises as a problem with the MT/AMT method. Three-dimensional earth modeling, now in progress,

may resolve these problems. If not, then the MT/AMT method may decline in application in geothermal exploration.

### Heat flow measurements

In order to examine the near-surface hydrothermal regime directly, we have measured temperatures in 40 drill holes varying in depth from 40 to 200 m. Thermal conductivity measurements were made on drill cores and cuttings so that a conductive heat flux could be computed for the upper section of each drill hole. A heat flow map representing this conductive heat loss is shown in Figure 14.

As typical Basin and Range heat flow values in western Utah fall between 75 and 100  $\text{mW m}^{-2}$  (1.8 and 2.4 HFU), the 100  $\text{mW m}^{-2}$  contour may be considered as the boundary for the near-surface geothermal system. Within this region, the clear correspondence between the heat flow contour shapes and the position of faults indicates the strong structural control on the system. Very high heat flow exceeding 1  $\text{W m}^{-2}$ , and attaining a maximum value of about 9  $\text{W m}^{-2}$  is found in a 2-km wide band parallel to and including the Opal Mound fault. Seven production wells have been drilled in this region. The northwest trend of the contours north of the Hot Springs fault may result from leakage or may indicate reservoir geometry. The variable and low heat flows in the central Mineral Mountains are likely associated with a recharge region.

The heat flow pattern is thus consistent with a hydrothermal system involving a region of hydrologic recharge in the Mineral Mountains, a reservoir associated with the eastward-dipping Opal Mound fault zone and a region of leakage westward into the Milford graben. However, the pattern by itself provides little constraint on the ultimate heat source for the system. We have therefore computed the magnitude of the present heat loss by integrating the heat flux over the areas bounded by heat flow contours in Figure 14. This total heat loss is 70 megawatt (MW). Allowing for reasonable contributions from (a) background basin and range level heat flow, (b) local hydrologic recharge and discharge, and (c) exothermic clay alteration reactions, the remaining heat loss, estimated at 60 MW, must be supplied by a source at depth. Using arguments similar to those employed by Lachenbruch et al (1976) for the Long Valley caldera, we estimate that this heat could be supplied by steady-state conduction from a source at a temperature near the granite solidus having lateral dimensions of the Mineral Mountains pluton at a depth of 7 km. The depth increases if hydrothermal



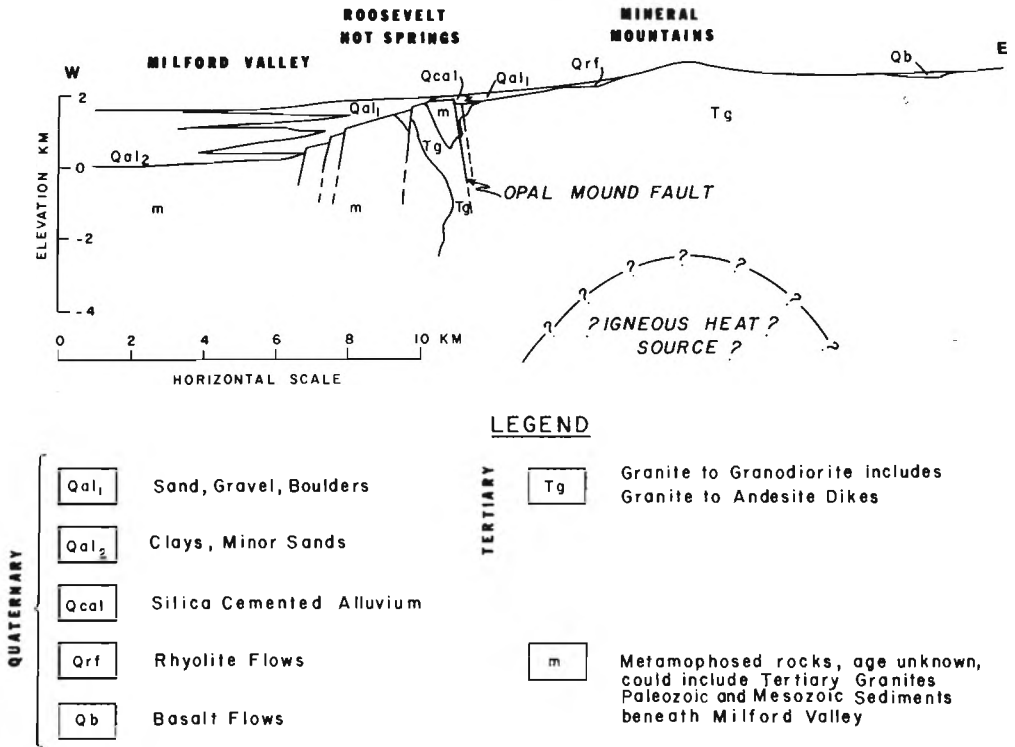


FIG. 15. Generalized east-west geologic cross-section through Roosevelt Hot Springs thermal area.

convection plays a significant role in transferring heat, and decreases if the lateral size of the source is diminished. If the present heat loss has been maintained since the emplacement of the rhyolite domes 0.5 m.y. ago, the quantity of heat involved necessitates a resupply of heat, possibly from deeper magmatic sources.

The heat loss of 70 MW should not be confused with the production potential of the system, which is considerably greater. The spatial pattern of successful drill holes, together with our surveys, suggests a conservative estimate of 10 km<sup>2</sup> for the size of a region that may be brought into production. This area will support about 60 production wells (1 well per 40 acres) which at 5 MW/well will yield 300 MW electricity.

### CONCLUSIONS

#### Delineation of the reservoir and its source of heat

Figure 15 portrays a generalized east-west geologic cross-section through the Roosevelt Hot Springs thermal area. Beneath Milford Valley, gravity data

suggest about 1400 m of Quaternary alluvium. Tertiary granite or Paleozoic and Mesozoic sediments could underlie the alluvium, although we indicate in Figure 15 that metamorphic rocks are the bedrock on this cross-section. The aeromagnetic data have not resolved bedrock type because of the great depth of valley fill. Refraction seismic data, now being processed and interpreted, will provide depth control on the gravity data, and a combination of density and velocity information might then permit us to identify whether Tertiary granite or Paleozoic or Mesozoic sediments are present in the section beneath Milford Valley.

The Opal Mound fault is the western boundary of a fracture zone estimated to be at least 0.5 km wide from the electrical data. However, producing fractures have been intersected as much as 1.5 km east of the Opal Mound fault. Although the dip of the fracture zone is not known, we show it as steeply dipping to the east (Figure 15). The true width of the zone is also unknown. Refraction and reflection seismic surveys are expected to be the best methods for resolving these unknown features.

The pronounced gravity saddle shown in Figure 7 and discussed earlier remains unexplained at present. Once the seismic refraction data have been used to control the gravity model of Figure 9, then the effect of the deep Milford Valley fill can be removed and the residual gravity studied to determine whether a buried low-density pluton is associated with the saddle. The small gravity lows labelled D and E in Figure 7 are modeled by low-density material no deeper than 2 km; we are reluctant to attribute to these small features a significance in terms of modern day heat flow. Thus, until we have seismic refraction control for the gravity data, we cannot infer with any confidence the occurrence of a deeply buried intrusion of low density which might serve as the source of heat. In Figure 15, we have, however, sketched in a location for an igneous heat source as a postulate which will be tested using the combined gravity and seismic refraction data. The aeromagnetic data might then be interpreted in a much more quantitative manner than heretofore possible.

The *P*-wave delay data provide only a tenuous suggestion of a partial melt. Additional *P*-wave delay studies, currently under way, may help to resolve the question of whether a partial melt or an intense fracture zone occurs at or near the location of the postulated igneous heat source.

MT/AMT data, if interpretation problems can be overcome, could detect by low resistivities a partial melt provided it contained substantial water (Lebedev and Khitarov, 1964). An intrusive equivalent of the rhyolite flows and domes would be satisfactory in this sense. A brine-saturated intensely fractured zone at several kilometers depth would be detected by the MT/AMT method, if its volume were as large as indicated by the postulated igneous heat source. A hot dry rock with no partial melt would not be detectable with MT/AMT. The above conclusions concerning MT/AMT are discussed in detail by Wannamaker et al (1978).

The igneous heat source could be the deeper part of the Tertiary granite pluton. Fractures extending to depths of several kilometers in a 10 m.y. old pluton might tap an unusually steep thermal gradient. This and other models of the geothermal system are being used in combined conductive-convective heat flow studies, but no results are yet available.

We are continuing our modeling of the various data sets available to us. Light, stable isotopes can provide an estimate of the amount of water interacting with a given volume of rock and on the source of the water. This knowledge, combined with hydrologic and structural studies, may provide some notion of

the size of the fracture system. Better control for modeling geophysical data sets is expected to result. For the moment we must conclude that we know little about the deep internal characteristics of the geothermal system.

### Exploration procedure

A great deal of effort has obviously been expended in an attempt to document and understand the Roosevelt Hot Springs thermal area. While the documentation is proceeding apace, the understanding is lagging. Given this situation, it is fair to ask how this case history can aid, in general, the search for this class of geothermal field. We shall attempt in the following to provide some guidelines.

**Phase 0—Office study.**—At the outset of any exploration campaign, one assembles, synthesizes, and digests all of the available information for an area or a prospect (Ward, 1977). Data to be studied include local and regional geology, geophysics, geochemistry, geography, and hydrology. The possibility of economic viability of the prospect or area then emerges.

**Phase 1—Remote sensing.**—The available photographic imagery is usually inadequate for either prospect or area delineation. Attempts to use infrared imagery have, perhaps surprisingly, failed to assist in a significant way because of the enormous signal-to-noise ratio problems associated with the superposition of the diurnal cycle, the hydrological regime, the topographic effects, and other environmental factors. Hence, low sun-angle photography and vertical illumination color photography have been used routinely while infrared techniques were tested only superficially. We recommend low sun angle black-and-white photography, which has been the most useful to us.

**Phase 2—Reconnaissance field activities.**—Reconnaissance field exploration follows assembly and analyses of available data sets and imagery. Based upon our experiences, we recommend regional geologic mapping to establish the validity of the previous studies and to set a framework for the subsequent portions of the exploration sequence. In the eastern basin and range physiographic province, the occurrence of relatively young rhyolites (<1.0 m.y.) and/or of relatively young granitic plutons (<1.0 m.y.) appears to be essential to the occurrence of high temperature (>200°C) geothermal resources. Geothermal resources of lower temperature seem to involve circulation of meteoric water to 2 to 5 km depths in *normal* geothermal gradients. Hence, radiometric dating of all extrusive and intrusive acidic

rocks is essential to assessment of geothermal resources of a region. Basalt flows of less than 10,000 yr. might also leave fingerprints on the current heat flow patterns requiring dating of them.

In this same phase Na-K-Ca, SiO<sub>2</sub>, and isotopic geothermometry of water as potential indicators of subsurface temperatures ought to be considered; the former two geothermometers are diagnostic of a high-temperature geothermal resource in the Roosevelt Hot Springs thermal area.

Regional aeromagnetic and gravity surveys at the Roosevelt Hot Springs thermal area have proved useful in locating faults, in identifying rock units, and in estimating depth of valley fill. These inexpensive methods, therefore, aid in our understanding the general structure of the area under study. Whether they can be diagnostic of the presence of geothermal resources in the eastern Basin and Range province has yet to be established.

Regional collection of thermal gradients in available water wells, mining exploration drill holes, and oil and gas wells can hardly be disputed as a major exploration tool; it is inexpensive and directly indicative of the resource sought—heat.

**Phase 3—Heat flow measurements in strategically located drill holes.**—The fundamental property to be observed in exploration for geothermal resources is heat flow. How best to observe heat flow is a question of the most profound significance, since hot thermal waters convect upwards, hot intrusions drive this mechanism but also produce conductive heat flow outwards, and cool meteoric waters commonly obscure both effects from surface observation. Nevertheless, it seems to us that the heat flow pattern at the Roosevelt Hot Springs thermal area is basically diagnostic of a high-temperature geothermal resource. Unfortunately, the drilling target is not delineated since three nonproductive wells, as well as seven productive wells, all occur within the area of exceptionally high heat flow.

**Phase 4—Electrical methods.**—We observe from Figures 11, 12, and 13 that electrical resistivity surveys define the fracture system of the Roosevelt Hot Springs thermal area very well, especially when guided by geology, photogeology, and aeromagnetics. While not shown here, we are aware that bipole-dipole surveys are not effective in delineating the fault system. We have found dipole-dipole surveys, augmented by Schlumberger and shallow electromagnetic surveys, to be the most effective in this area.

**Phase 5—Petrological, mineralogical and geochemical studies on cuttings and cores from heat flow drill holes.**—Only by detailed petrological, mineralogical, and geochemical studies of cuttings and cores, plus chemical studies on brines, have we been able to establish that the shallow low resistivities over the geothermal reservoir arise primarily as a result of clay alteration and, to a lesser extent, to the presence of a 7000 ppm TDS brine. For this reason alone, petrological, mineralogical, and geochemical studies on cuttings and cores obtained in holes drilled for heat flow measurements are essential. Of possibly greater importance, they provide an indicator of past and present temperature-pressure regimes to which the reservoir has been subject. The importance of such studies has been illustrated in the body of this paper.

**Phase 6—Model test drilling.**—Arguments can be raised in favor of drilling deep test wells at this juncture in the exploration sequence. The cost of a 2000-m well, if productive, would be about \$800,000 and if nonproductive would be about \$600,000. Slim hole model test wells at a cost of \$200,000 for a depth of 700 m are often preferred. One discovery well and three proof wells are required to establish a discovery. Full petrological, mineralogical, chemical, and isotopic analyses of well cuttings, cores, and fluids are required for understanding the geothermal system. We have only partially demonstrated the importance of these studies in this manuscript.

**Phase 7—Detailed seismic refraction and reflection surveys.**—We have not yet demonstrated that detailed seismic refraction and reflection surveys will contribute to our understanding of the Roosevelt Hot Springs reservoir and its source of heat. Yet any further significant advance in our understanding of this geothermal system seems to be dependent upon the intelligent use of these methods. For this reason we include them here.

**Phase 8—Modeling and synthesis of all available data.**—The weakest part of this case history is our inability to model any data set adequately, but more importantly, we are unable to synthesize an overall model of the geothermal system from our current efforts at multiple data set modeling. Much effort is required in this direction if we are to develop a cost-effective exploration architecture suited to detection and delineation of high-temperature geothermal resources in the eastern basin and range physiographic province.

## EPILOGUE

We have yet to find useful applications of the earth noise, microearthquake, *P*-wave delay, magnetotelluric, and self-potential methods in this complex geologic setting. Nevertheless, we are continuing to study these methods. Thirty years ago, mining geophysical exploration was in the same state of uncertainty but has matured substantially since then. Whither thou, geothermal geophysical exploration? After four years of intensive study of the Roosevelt Hot Springs thermal area, we have learned of the general locations of the fracture systems which allow cold meteoric fluid flow to depth and of hot thermal fluid flow to surface. The data reported here have helped industry in locating wells but have not prevented drilling of four nonproductive wells. Data currently being analyzed are expected to provide significant improvement in our model of the subsurface. However, many problems will remain.

Specific problems requiring pure and applied research include (a) means for detecting and delineating fault systems in which thermal fluids percolate; (b) means for evaluating the size, productivity, and longevity of a fracture-dominated geothermal reservoir; (c) means for identifying the fluid-rock interactions which lead to heat flow to surface; and (d) means for identifying the source of heat. These are difficult problems to solve.

## ACKNOWLEDGMENTS

We are grateful for reviews of drafts of this paper by Gary W. Crosby, David D. Blackwell, M. G. Best, and W. H. Duffield. Financial support, permitting the research on which this summary paper is based, was received under Grant no. GI 43741 of the RANN program from the National Science Foundation and under Contract no. EY-76-S-07-1601 from the Division of Geothermal Energy of the Energy Research and Development Administration, now the Department of Energy. We are indebted to all industrial concerns with lease holdings in the area for cooperation in the conduct of our surveys: Special thanks are due in this respect to Phillips Petroleum Co. and Thermal Power Co. We are indebted to the many students who participated in the research. J. M. Bodell, W. D. Brumbaugh, J. A. Carter, T. J. Crebs, T. L. Olson, I. Thangsuphanich, A. C. Tripp, and P. E. Wannamaker contributed substantially to the geophysical data and interpretation. N. L. Bryant, R. E. Dedolph, S. H. Evans, Jr., and D. Bowers added materially to geology, geochemistry, and igneous petrology.

## REFERENCES

- Armstrong, R. L., 1970, Geochronology of Tertiary igneous rocks, eastern Basin and Range province, western Utah, eastern Nevada, and vicinity, U.S.A.: *Geochim. Cosmochim. Acta*, v. 34, p. 203-232.
- Brown, F. H., 1977, Attempt at paleomagnetic dating of opal, Roosevelt Hot Springs KGRA: *Tech. Rep. v. 77-1*, DOE/DGE contract EY-76-S-07-1601, Univ. of Utah, 13 p.
- Brumbaugh, W. D., and Cook, K. L., 1977, Gravity survey of the Cove Fort—Sulphurdale KGRA and the North Mineral Mountains area, Millard and Beaver Counties, Utah: *Tech. Rep. v. 77-4*, DOE/DGE contract EY-76-S-07-1601, Univ. of Utah, 131 p.
- Bryant, N. L., and Parry, W. T., 1977, Hydrothermal alteration at Roosevelt Hot Springs KGRA—DDH 1976-1: *Tech. Rep. v. 77-5*, DOE/DGE contract EY-76-S-07-1601, Univ. of Utah, 131 p.
- Carter, J. A., and Cook, K. L., 1978, Regional gravity and aeromagnetic surveys of the Mineral Mountains and vicinity, Millard and Beaver Counties, Utah: *Final rep. v. 77-11*, DOE/DGE contract EY-76-S-07-1601, Univ. of Utah, 179 p.
- Crebs, T. L., and Cook, K. L., 1976, Gravity and ground magnetic surveys of the central Mineral Mountains, Utah: *Final rep. v. 6*, NSF grant GI-43741, Univ. of Utah, 129 p.
- Dedolph, R. E., and Parry, W. T., 1976, A thermodynamic model of the hydrolysis of microcline: *Tech. rep. v. 76-2*, DOE/DGE contract EY-76-S-07-1601, Univ. of Utah.
- Eaton, G. P., Wahl, R. R., Prostka, H. J., Mabey, D. R., and Kleinkef, M. D., 1978, Regional gravity and tectonics patterns: Their relation to late Cenozoic epeirogeny and lateral spreading in Western Cordillera: *Memoir 152*, GSA, editors, R. B. Smith and G. P. Eaton, *Cenozoic tectonics and regional geophysics of the Cordillera*.
- Evans, S. H., Jr., 1977, Geologic map of the central and northern Mineral Mountains, Utah: *Tech. rep. v. 77-7*, DOE/DGE contract EY-76-S-07-1601, Univ. of Utah.
- Evans, S. H., Jr., and Nash, W. P., 1978, Quaternary rhyolite from the Mineral Mountains, Utah, U.S.A.: *Final rep. v. 77-10*, DOE/DGE contract EY-76-S-07-1601, Univ. of Utah, 59 p.
- Fournier, R. O., and Truesdell, A. H., 1974, Geochemical indicators of subsurface temperature—Part 2: Estimation of temperature and fraction of hot water mixed with cold water: *U.S.G.S.J. Res.*, v. 2, p. 263-270.
- Geotronics Corp., 1976, Magnetotelluric survey and resistivity maps, Roosevelt Hot Springs, Utah: *Final rep. v. 5*, DOE/DGE contract EY-76-S-07-1601, 5 maps, Univ. of Utah.
- Helgeson, H. C., 1968, Evaluation of irreversible reactions in geochemical processes involving minerals and aqueous solutions—I. Thermodynamic relations: *Geochim. et Cosmochim. Acta*, v. 32, p. 853-877.
- 1969, Thermodynamics of hydrothermal systems at elevated temperatures and pressures: *Am. J. Sci.*, v. 267, p. 729-804.
- Hemley, J. J., Hostetler, P. B., Gude, A. J., and Mountjoy, W. T., 1969, Some stability relations of alunite: *Econ. Geol.*, v. 64, p. 599-612.
- Hildreth, E. W., 1977, The magma chamber of the Bishop tuff: Gradients in temperature, pressure, and composition: *Ph.D. thesis*, Univ. Calif., Berkeley.
- Lachenbruch, A. H., Sorey, M. L., Lewis, R. E., and Sass, J. H., 1976, The near-surface hydrothermal regime of Long Valley Caldera: *J. Geophys. Res.*, v. 81, p. 763-769.
- Lebedev, E. B., and Khitarov, N. I., 1964, Dependence on the beginning of melting of granite and the electrical

- conductivity of its melt on high water vapour pressure: *Geokhimiya*, no. 3, p. 195-201.
- Lipman, P. W., Rowley, P. D., Mehnert, H. H., Evans, S. H., Jr., Nash, W. P., and Brown, F. H., 1977. Pleistocene rhyolite of the Mineral Range, Utah: geothermal and archeological significance: *U.S.G.S. J. Res.*, v. 6, no. 1, p. 133-147.
- MicroGeophysics, Inc., 1977. Refraction shooting near Roosevelt Hot Springs: Data, final rep., v. 77-4, DOE/DGE contract EY-76-S-07-1601, Univ. of Utah., 56 p.
- Mundorff, J. C., 1970. Major thermal springs of Utah: *Utah Geol. and Mineral Survey Water Resources Bull.* 13, 60 p.
- Nash, W. P., 1976. Petrology of the Quaternary volcanics of the Roosevelt KGRA, and adjoining area, Utah: Final rep., v. 1, NSF grant GI-43741, Univ. of Utah, 95 p.
- Nash, W. P., and Evans, S. H., Jr., 1977. Natural silicic liquids: fugacities and flow: *GSA Abstr. with programs*, v. 9, no. 7, p. 1110.
- Norrish, K., and Hutton, J. T., 1969. An accurate X-ray spectrographic method for the analysis of a wide range of geologic samples: *Geochim. et Cosmochim. Acta*, v. 33, p. 431-454.
- Olson, T. L., and Smith, R. B., 1976. Earthquake surveys of the Roosevelt Hot Springs and the Cove Fort areas, Utah: Final rep., v. 4, NSF grant GI-43741, Univ. of Utah, 83 p.
- Park, G. M., 1971. Volcanics, Thomas Range, in *Radioactive and isotopic age determinations of Utah rocks*: *Utah Geol. and Mineral Survey Bull.* 81.
- Parry, W. T., Benson, N. L., and Miller, C. D., 1976. Geochemistry and hydrothermal alteration at selected Utah hot springs: Final rep. v. 3, NSF grant GI-43741, Univ. of Utah, 131 p.
- Schoen, R., White, D. E., and Hemley, J. J., 1974. Argillization by descending acid at Steamboat Springs, Nevada: *Clays and clay minerals*, v. 22, p. 1-22.
- Sill, W. R., and Bodell, J., 1977. Thermal gradients and heat flow at Roosevelt Hot Springs: Tech. rep., v. 77-3, DOE/DGE contract EY-76-S-07-1601, Univ. of Utah, 63 p.
- Sill, W. R., and Ward, S. H., 1978. Electrical energizing of well casings: Final rep., v. 77-8, DOE/DGE contract EY-76-S-07-1601, Univ. of Utah, 10 p.
- Smith, R. B., 1977. Long-term seismic monitoring of the Roosevelt—Cove Fort KGRA's: Final rep., v. 77-3, DOE/DGE contract EY-76-S-07-1601, Univ. of Utah.
- Smith, R. B., and Sbar, M., 1974. Contemporary tectonics and seismicity of the western states with emphasis on the Intermountain Seismic Belt: *GSA Bull.*, v. 85, p. 1205-1218.
- Stokes, W. L., 1968. Relation of fault trends and mineralization, eastern great basin, Utah: *Econ. Geol.*, v. 63, p. 751-759.
- Sykes, L. R., 1970. Earthquake swarms and seafloor spreading: *J. Geophys. Res.*, v. 75, p. 6598-6611.
- Thangsuphanich, I., 1976. Regional gravity survey over the southern Mineral Mountains, Beaver County, Utah: M.S. thesis, Univ. of Utah.
- Tripp, A. C., Ward, S. H., Sill, W. R., Swift, C. M., Jr., and Petrick, W. R., 1978. Electromagnetic and Schlumberger resistivity sounding in the Roosevelt Hot Springs KGRA: *Geophysics*, this issue, p. 1450-1469.
- Wannamaker, P. E., 1978. Magnetotelluric investigations at Roosevelt Hot Springs and Mineral Mountains area, Utah: Topical rep., v. 78-1701.a.6.i, DOE/DGE contract EY-78-S-07-1701, Univ. of Utah, 53 p.
- Wannamaker, P. E., Sill, W. R., and Ward, S. H., 1978. Magnetotelluric investigations at the Roosevelt Hot Springs KGRA and Mineral Mountains, Utah: *Proc., G.R.C. ann. meeting*, Hilo, Hawaii.
- Ward, S. H., 1977. Geothermal exploration architecture: Tech. rep., v. 77-2, DOE/DGE contract EY-76-S-07-1601, Univ. of Utah, 20 p.
- Ward, S. H., and Crebs, T., 1975. Report on preliminary resistivity survey, Roosevelt Hot Springs KGRA: NSF grant GI-43741, Univ. of Utah, 5 p.
- Ward, S. H. and Sill, W. R., 1976a. Dipole-dipole resistivity surveys, Roosevelt Hot Springs KGRA: NSF final rep., v. 2, grant GI-43741, Univ. of Utah, 29 p.
- 1976b. Dipole-dipole resistivity delineation of the near-surface zone at the Roosevelt Hot Springs Area: Tech. rep. 76-1, contract EY-76-S-07-1601, Univ. of Utah, 7 p.
- White, D. E., 1957. Magmatic, connate, and metamorphic waters: *GSA Bull.*, v. 68, p. 1659-1682.
- 1970. Geochemistry applied to discovery, evaluation, and exploitation of geothermal energy resources: *Rapporteur's rep., UN Sympos. on Development and Utilization of Geothermal Resources, Pisa Proc., (Geothermics, spec. iss. 2) v. 1, p. 58-80.*